

Revisiting Randomization in Greedy Model Search

Xin Chen* Jason M. Klusowski* Yan Shuo Tan† Chang Yu*

Abstract

Combining randomized estimators in an ensemble, such as via random forests, has become a fundamental technique in modern data science, but can be computationally expensive. Furthermore, the mechanism by which this improves predictive performance is poorly understood. We address these issues in the context of sparse linear regression by proposing and analyzing an ensemble of greedy forward selection estimators that are randomized by feature subsampling—at each iteration, the best feature is selected from within a random subset. We design a novel implementation based on dynamic programming that greatly improves its computational efficiency. Furthermore, we show via careful numerical experiments that our method can outperform popular methods such as lasso and elastic net across a wide range of settings. Next, contrary to prevailing belief that randomized ensembling is analogous to shrinkage, we show via numerical experiments that it can simultaneously reduce training error and degrees of freedom, thereby shifting the entire bias-variance trade-off curve of the base estimator. We prove this fact rigorously in the setting of orthogonal features, in which case, the ensemble estimator rescales the ordinary least squares coefficients with a two-parameter family of logistic weights, thereby enlarging the model search space. These results enhance our understanding of random forests and suggest that implicit regularization in general may have more complicated effects than explicit regularization.

Keywords: Regression; Forward Selection; Greedy Model Search; Random Forests; Ensemble Learning

1 Introduction

Sparse linear regression is a well-studied problem in statistics, having important applications to machine learning, signal processing, and other fields. Given a response vector $\mathbf{y} = (y_1, y_2, \dots, y_n)^\top$ and data matrix $\mathbf{X} = [\mathbf{x}_1 \ \mathbf{x}_2 \ \dots \ \mathbf{x}_n]^\top$, this problem is traditionally framed as best subset selection (BSS) [5, 35], which seeks to minimize $\|\mathbf{y} - \mathbf{X}\boldsymbol{\beta}\|^2 = \frac{1}{n} \sum_{i=1}^n (y_i - \mathbf{x}_i^\top \boldsymbol{\beta})^2$ subject to $\|\boldsymbol{\beta}\|_{\ell_0} \leq k$, where $\|\boldsymbol{\beta}\|_{\ell_0}$ measures the number of nonzero entries in $\boldsymbol{\beta}$. Since exactly solving the BSS problem is computationally infeasible, early approaches

*Department of Operations Research and Financial Engineering, Princeton University

†Department of Statistics and Data Science, National University of Singapore

to sparse linear regression comprised greedy search (GS) algorithms, such as forward selection (FS) [22], matching pursuit (MP) [62], and orthogonal matching pursuit (OMP) [20]. These algorithms iteratively select features that maximize the immediate reduction in mean squared error or a proxy thereof. In recent years, however, greedy methods have been largely supplanted by the lasso [51], elastic net [63], and other convex relaxation techniques [26, 34]. This shift stems from the fact that, compared to greedy methods, convex relaxation approaches typically offer stronger theoretical guarantees under milder assumptions [52, 14, 55, 12, 34] and often demonstrate superior empirical performance [51, 63, 32, 12].

Breiman hypothesized in 1996 [8] that greedy methods may suffer from instability [59]—small changes in \mathbf{y} or \mathbf{X} can cause drastic differences in selected features and resulting models—leading to high variance in cross-validation performance estimates and making hyperparameter tuning especially challenging. To address this issue, he proposed stabilizing greedy methods through randomized ensembling, which involves averaging the predictions from multiple estimators, each obtained by applying a greedy method to a perturbed version of the dataset. He investigated perturbation techniques such as bootstrap resampling (“bagging”) and adding noise to the response (“smearing”), and showed empirically, as well as to some extent theoretically, that they led to better stability and prediction performance [7, 8, 9]. However, these randomized ensemble methods did not seem to outperform convex relaxation approaches and were further limited by their high computational cost. They have hence not gained popularity in a sparse linear regression context. On the other hand, when adapted to the setting of nonlinear estimators, such as via random forests (RFs), these ensembling techniques have proved to be wildly successful [10, 15, 27, 45]. The exact reasons for their success remains somewhat elusive and an active topic of research [13, 56, 43, 37, 48, 47, 46, 23, 19, 40, 41, 49].

In this paper, we revisit randomized ensembling of greedy methods in sparse linear regression, with the dual objective of (i) developing a state-of-the-art method for solving sparse linear regression and (ii) explaining the general success of randomized ensembling. We utilize a different type of data perturbation—at each iteration of the greedy method, we select a random subset of m features and select the best feature from within this subset. We call this *feature subsampling* and note that a version of this scheme is used in RFs. We show that, when used with FS, randomized ensembling via feature subsampling overcomes some of the computational limitations of bagging and smearing, while enjoying marked prediction performance improvements. This success leads us to call this ensembling method *Randomized Greedy Search (RGS)*. More precisely, we design a dynamic programming implementation of RGS whose computational complexity can, under some circumstances, scale sublinearly in the number of estimators in the ensemble. Together with its synergy with modern parallel and distributed computing paradigms, this dynamic programming framework helps bridge the computational efficiency gap between randomized ensembling and convex relaxation methods. Meanwhile, through extensive experiments on synthetic data, we show that the prediction performance of RGS is comparable with that of convex relaxation methods and even surpasses them under certain settings, such as low signal-to-noise ratio or banded correlated features.¹

¹RGS is implemented in our fully fledged package github.com/yuyumi/RGS with an sklearn-compatible

We argue that the reasons for the predictive effectiveness of RGS go beyond Breiman’s earlier hypothesis of stabilization [8] or his later explanation of variance reduction [10]. Instead, *RGS, and randomized ensembling more broadly, serves to enlarge the model space being searched over, thereby shifting the entire bias-variance trade-off curve.* Indeed, for a fixed number of greedy search iterations k , we show empirically that RGS often has a smaller training error compared to its non-ensembled version (GS), while simultaneously having smaller degrees of freedom, which is a measure of the gap between training and test error. We are able to make this argument even more precise through theoretical analysis. Following a longstanding precedent in statistics, we focus on the case of orthogonal features, under which FS, MP, and OMP are all equivalent to BSS. In this setting, we show RGS adaptively reweights ordinary least squares (OLS) coefficients, creating a smooth approximation to the hard thresholding utilized by BSS. These weights are well-approximated by a logistic function in the OLS coefficient rankings, with inflection point roughly equal to k and growth rate depending on the feature subsampling ratio $\gamma := m/p$. Varying γ for a fixed k thereby searches over a larger space of models compared to BSS. Our first main theoretical result is a lower bound on the resulting decrease in training error in terms of the OLS coefficients. Meanwhile, our second main result identifies a sufficient concavity condition on the OLS coefficients for when RGS is guaranteed to have fewer degrees of freedom compared to BSS for the same value of k .

The rest of this paper is organized as follows. We describe RGS and its efficient implementation in Section 2. We present our main theoretical results regarding the reduction in training error and degrees of freedom from feature subsampling in Section 3 and our numerical experiments in Section 5. Further results on the properties of RGS weights are shown in Section 4. In Section 6, we discuss how our theoretical results add clarity to the debate regarding the role of randomization in the success of RFs [56, 43, 19, 40, 41, 49]. Specifically, while previous work argued that feature subsampling works by “regularizing” RFs, our work supports the claim that it can also reduce bias by enlarging the model search space. In Section 7, we conclude with a discussion of the limitations of our study and potential future work.

2 Randomized Greedy Search

In this section, we formally introduce our proposed method, RGS, for solving sparse linear regression. Note that such a method has generality beyond linear modeling, as one can make use of a dictionary of derived features, which could consist of, for example, trigonometric, spline, wavelet, radial, or ridge functions. Such features can either be defined using prior knowledge, or even learned from data. For conceptual simplicity, however, we use the former framing for the rest of this paper. The inner product between two vectors $\mathbf{a}, \mathbf{b} \in \mathbb{R}^n$ is defined as $\langle \mathbf{a}, \mathbf{b} \rangle = (\mathbf{a}^\top \mathbf{b})/n$, with norm $\|\mathbf{a}\|^2 = (\mathbf{a}^\top \mathbf{a})/n$. We denote the j -th feature vector in bold as $\mathbf{x}_{j,p} := (x_{1j}, x_{2j}, \dots, x_{nj})^\top$ and assume it is normalized so that $\|\mathbf{x}_{j,p}\| = 1$. Functions, such as the j -th coordinate function $x_{j,p}$, will be denoted in regular font.

API. Code for reproducing all of the results in this paper is also available in the same package.

2.1 Forward Selection

We first describe FS, which is the default base learner used by RGS. Starting with an empty active set $\mathcal{M}_0 = \emptyset$ and iterating over $l = 1, 2, \dots, k$ for some prespecified sparsity level k , it updates \mathcal{M}_{l-1} with the feature indexed by

$$\begin{aligned} j_l &:= \arg \min_{j \in \mathcal{V}_l} \|\mathbf{y} - \mathbf{P}_{\mathcal{M}_{l-1} \cup \{j\}} \mathbf{y}\| \\ &= \arg \max_{j \in \mathcal{V}_l} \frac{|\langle \mathbf{r}_{l-1}, \mathbf{x}_{j,p} \rangle|}{\|\mathbf{P}_{\mathcal{M}_l}^\perp \mathbf{x}_{j,p}\|}, \end{aligned} \tag{1}$$

and sets the updated model predictions to be $\hat{\mathbf{f}}_{l,p} := \mathbf{P}_{\mathcal{M}_l} \mathbf{y}$. Here, $\mathbf{P}_{\mathcal{M}_l}$ (resp. $\mathbf{P}_{\mathcal{M}_l}^\perp$) denotes the projection matrix onto the (resp. orthogonal complement of the) column span of the feature vectors indexed in \mathcal{M}_l , $\mathbf{r}_{l-1} := \mathbf{y} - \hat{\mathbf{f}}_{l-1,p}$ denotes the vector of residuals at the $(l-1)$ -th step, and $\mathcal{V}_l = [p] \setminus \mathcal{M}_{l-1}$. We use $\hat{f}_{k,p}$ to denote the predictive function obtained after k steps, henceforth called the FS estimator.

FS is of course not the only greedy search algorithm. Notable alternatives include OMP, which does not project out the contributions from $\mathbf{x}_{j,p}$ in (1) and instead just uses the absolute correlation of \mathbf{r}_{l-1} with $\mathbf{x}_{j,p}$, and MP, which uses the same objective as OMP, but updates the model predictions via $\hat{\mathbf{f}}_{l,p} = \hat{\mathbf{f}}_{l-1,p} + \langle \mathbf{r}_{l-1}, \mathbf{x}_{j,p} \rangle \mathbf{x}_{j,p}$ and allows the same feature to be selected multiple times. When efficiently implemented, all three algorithms have similar computational complexity. In particular, FS can be implemented by maintaining a QR factorization of the active submatrix $\mathbf{X}_{\mathcal{M}_l}$, which can be updated with a rank-one modification upon adding a new selected variable. At step l , the computational cost is $O(np)$ for computing (1), $O(nl)$ for updating the QR factorization, and $O(n)$ for updating the residuals. Summing over k steps gives a total cost of $O(npk)$. Since $k \leq \min\{n, p\}$, this cost is no more than that of a single OLS fit.

2.2 Randomized Greedy Search

Our proposed RGS estimator comprises an ensemble of randomized FS estimators.² Each FS estimator is randomized at each step l by modifying (1) to instead select the maximizer over $j \in \mathcal{V}_l$, where \mathcal{V}_l , called the candidate set, is now a subset of size m drawn uniformly at random from $[p] \setminus \mathcal{M}_{l-1}$.³ Stopping at k steps as before, we call the resulting estimator $\tilde{f}_{k,p,b}$. We repeat this model building process across B independent replicates, and aggregate the resulting estimators via simple averaging to get the RGS estimator $\hat{f}_{k,m,p,B} := B^{-1} \sum_{b=1}^B \tilde{f}_{k,p,b}$. Recall that we call this randomization scheme feature subsampling, and note that it differs from bagging and smearing in that the randomization is interleaved with optimization via the modified (1), whereas bagging and smearing make use of a one-off dataset randomization prior to running FS.

²We call our method RGS because the base learner can be easily replaced with other GS methods, and can be further generalized to GS methods for nonlinear models.

³If $|\mathcal{V}_l| < m$, we do not randomize.

2.3 Efficient RGS via Dynamic Programming

If computed naively, the computational cost of RGS scales linearly in B , the number of replicates. Since it is standard to take B to be in the hundreds (or thousands) in order to minimize the contribution of algorithmic variance to prediction error, this could potentially make RGS prohibitively expensive. Fortunately, we are able to design an efficient dynamic programming implementation of RGS that significantly reduces the computational overhead.

Our method leverages the observation that the same active set may appear across multiple replicates, which means that much computation is needlessly repeated. To avoid this waste, we run all replicates simultaneously, maintaining, at the start of each step l , an object \mathcal{S}_{l-1} , comprising all unique subsets of size $l-1$ selected at the previous step, as well as the number of times each subset occurs. To update \mathcal{S}_{l-1} , we process each entry $(\mathcal{M}, B_{\mathcal{M}})$ as follows: We generate B candidate sets $\mathcal{V}^{(1)}, \mathcal{V}^{(2)}, \dots, \mathcal{V}^{(B)} \subset [p] \setminus \mathcal{M}$ uniformly at random. To solve (1) for all candidate sets, we need only compute the correlations of the residual with features in $\cup_{b=1}^B \mathcal{V}^{(b)}$, and likewise for the feature projections, just once in total. Updating \mathcal{M} with these results provides B new, possibly repeated active sets $\mathcal{M}^{(1)}, \mathcal{M}^{(2)}, \dots, \mathcal{M}^{(B)}$, which we then return as a list (see also Figure 1). After processing all entries in \mathcal{S}_{l-1} in this manner, we concatenate all the resulting lists and count frequencies to get \mathcal{S}_l . After k steps, the RGS estimator can then be recovered as $\hat{f}_{k,m,p,B} = B^{-1} \sum_{(\mathcal{M}, B_{\mathcal{M}}) \in \mathcal{S}_k} B_{\mathcal{M}} \tilde{f}_{\mathcal{M}}$, where $\tilde{f}_{\mathcal{M}}$ is the OLS estimator given the data matrix $\mathbf{X}_{\mathcal{M}}$.

For $l = 1, 2, \dots, k$, let $\phi(l, m, B)$ denote the expected cardinality of \mathcal{S}_l . Arguing similarly to FS, the computational cost for handling each active set is $O(np)$. The total cost for our RGS implementation is thus $O(np \sum_{l=1}^k \phi(l, m, B))$, which can be much smaller than the naive $O(nmkB)$. We may further reduce the computational cost by repeatedly resampling \mathcal{S}_l before processing it. That is, we treat \mathcal{S}_l as a sample of size B from a population whose elements are subsets and repeatedly replace \mathcal{S}_l with a bootstrap resample of itself. Similar to the regular bootstrap, this progressively reduces the number of distinct elements in \mathcal{S}_l , while preserving the property that \mathcal{S}_l is an unbiased estimate of the original.

Remark. It is easy to see that this efficient implementation is unique to RGS, and is unavailable to other ensemble methods, which rely on perturbing data, and tend not to produce repeated calculations across replicates. It is also for this reason that we do not combine feature subsampling with bootstrapping, as practiced in RFs. We also note that there are limits to the efficiency gain in edge case hyperparameter choices (i.e., very small m or large k).

2.4 Prior Research on Feature Subsampling

The idea of combining models that are randomized via feature subsampling was first introduced by Breiman in the context of RFs [10]. It has since been applied in various statistical problems, such as linear regression [37], M-estimation [57], feature importance uncertainty estimation [29], clustering [28], and graph learning [58]. Most closely related to ours are two works that analyze feature subsampling applied to greedy algorithms, which we describe in more detail.

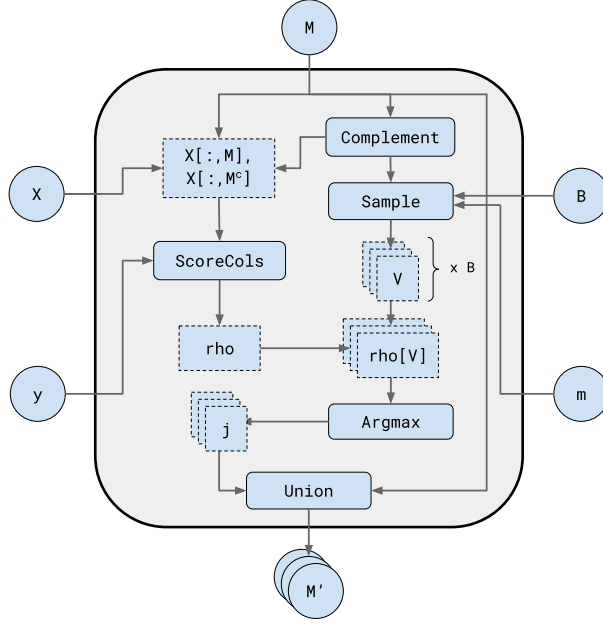


Figure 1: Diagram showing how the dynamic programming implementation of RGS processes an active set \mathcal{M} . It first uses (1) to compute scores for all columns of \mathbf{X} *not* in \mathcal{M} . Simultaneously, it generates B candidate subsets $\mathcal{V}^{(1)}, \mathcal{V}^{(2)}, \dots, \mathcal{V}^{(B)}$ of size m from the complement of \mathcal{M} . For within each candidate set, it then computes the index with the maximum score. \mathcal{M} is then updated with each of these values, returning a collection $\mathcal{M}^{(1)}, \dots, \mathcal{M}^{(B)}$.

Mentch and Zhou [43] introduce a version of RGS that incorporates bagging. However, their primary aim was to use it as a proxy to study RFs, and did not intend their method to be of practical use. Notably, they did not mention the efficient dynamic programming strategy that we introduced, nor did they provide any theoretical analysis. We will explain their arguments further in Section 6 when we discuss connections of our work to RFs. Separately, Zhan, Zhang, and Xia [60] propose ensemble projection pursuit regression, which applies feature subsampling to projection pursuit, a variant of greedy search that is essentially OMP with ridge-function dictionaries, without using bagging. While they obtain consistency rates for their method, they do not discuss the differences between the ensemble and non-ensemble versions. In particular, they do not show how randomized ensembling can shift the bias-variance trade-off curve.

3 Provable Error Reduction

3.1 Analytical Framework

In this section, we provide a theoretical explanation of the role of randomization in RGS. To do so, we assume a generative model $y_i = f(\mathbf{x}_i) + \varepsilon_i$, where $f(\mathbf{x}) = \boldsymbol{\beta}^\top \mathbf{x}$ is a linear function, $\varepsilon_1, \varepsilon_2, \dots, \varepsilon_n$ are IID noise variables with zero mean and variance σ^2 and that are

independent of the data matrix $\mathbf{X} \in \mathbb{R}^{n \times p}$.⁴

Our central claim is that randomization can simultaneously increase model fit and reduce model complexity, in contrast to earlier explanations. In a fixed design setting, the complexity of an estimator \hat{f} is often quantified via its *degrees of freedom* [32]:

$$\text{df}(\hat{f}) := \sum_{i=1}^n \frac{\text{Cov}(y_i, \hat{f}(\mathbf{x}_i))}{\sigma^2}.$$

Indeed, letting $\mathbf{f} = \mathbf{X}\boldsymbol{\beta}$ and $\hat{\mathbf{f}} = \mathbf{X}\hat{\boldsymbol{\beta}}$ denote the true and fitted function values respectively, the expected mean squared prediction error of \hat{f} can be decomposed into its expected training error and a constant multiple of its degrees of freedom; that is,

$$\mathbb{E}[\|\mathbf{f} - \hat{\mathbf{f}}\|^2] + \sigma^2 = \mathbb{E}[\|\mathbf{y} - \hat{\mathbf{f}}\|^2] + \frac{2\sigma^2}{n} \text{df}(\hat{f}). \quad (2)$$

Therefore, we will analyze how RGS compares to FS on each term on the right hand side of (2).

To aid our analysis, we make some simplifying assumptions. First, we study the performance of the method in the limit as $B \rightarrow \infty$. By the strong law of large numbers, the estimator $\hat{f}_{k,m,p,B}$ converges almost surely to its expected value, with the expectation taken over the randomness of the subset choice. For the rest of our theoretical discussion, we will use and refer to this large-limit model as the RGS estimator, denoting it as $\hat{f}_{k,m,p}$. In addition, we assume that the features are orthogonal:

Assumption 3.1 (Orthogonality). *The features are uncorrelated with respect to the sample, i.e., $\mathbf{X}^\top \mathbf{X}/n = \mathbf{I}$.*

While unlikely to describe most real datasets, Assumption 3.1 allows us to derive exact asymptotic expressions for coefficient behavior and precisely characterize how the randomization from feature subsampling propagates through the FS algorithm. This, in turn, enables direct comparisons with the broader regularization landscape, including ridge, lasso [51], elastic net [63], LARS [24], SCAD [26], MCP [61], and SureShrink [21], all of which have been studied in the orthogonal setting.

Remark. Note that FS, MP, OMP, and BSS are equivalent to each other under Assumption 3.1. In particular, this means that the error reduction that we demonstrate in this section has nothing to do with overcoming the failures of greedy optimization and everything to do with the suboptimal representation obtained via this class of ℓ_0 -penalized methods.

3.2 Coefficients and Weights

Let $\hat{f}_{\text{OLS}} = \sum_{j=1}^p \hat{\beta}_{j,p} x_{j,p}$ denote the ordinary least squares (OLS) estimator for f . Under Assumption 3.1, it is easy to see that its coefficients can be expressed as inner products $\hat{\beta}_{j,p} = \langle \mathbf{y}, \mathbf{x}_{j,p} \rangle$. It turns out that both the FS and RGS estimators can be written in terms

⁴Strictly speaking, we do not need to assume a well-specified linear model for our main results to hold, but we do so here for simplicity.

of the OLS coefficients. For ease of notation, we establish an ordering convention for the features $x_{1,p}, x_{2,p}, \dots, x_{p,p}$ in terms of these coefficients.

Definition 3.1 (Feature Ordering). The inner products $\hat{\beta}_{j,p} := \langle \mathbf{y}, \mathbf{x}_{j,p} \rangle$ are indexed and sorted by magnitude in descending order; that is,

$$|\hat{\beta}_{1,p}| \geq |\hat{\beta}_{2,p}| \geq \dots \geq |\hat{\beta}_{p,p}|. \quad (3)$$

For the sake of simplicity, we assume henceforth that there are no ties in the feature rankings, i.e., the inequalities in (3) are strict. Note also that the definition implies that the feature ordering is random as it depends on the response noise.

Using Definition 3.1 together with the equivalence of FS and BSS, we can write the k -step FS estimator as

$$\hat{f}_{k,p} = \sum_{j=1}^p \mathbf{1}(j \leq k) \hat{\beta}_{j,p} x_{j,p}, \quad (4)$$

which recounts the familiar fact that, in the orthogonal setting, FS (and BSS) will select the top- k features most correlated with the response. The indicators $\mathbf{1}(j \leq k)$ can be thought of as weights that modulate the OLS solution. Similarly, the k -step RGS estimator has the form

$$\hat{f}_{k,m,p} = \sum_{j=1}^p w_j^{k,m,p} \hat{\beta}_{j,p} x_{j,p}. \quad (5)$$

The RGS weights $w_1^{k,m,p}, w_2^{k,m,p}, \dots, w_p^{k,m,p}$ form a non-increasing sequence that takes values between 0 and 1 and which sum to k , i.e., the effective number of variables of the model. Furthermore, they are determined solely by structural parameters (j, k, m, p) rather than the actual coefficient values $\hat{\beta}_{j,p}$. In fact, as $m, p \rightarrow \infty$ with a fixed scaling ratio, they are closely approximated by a logistic function with midpoint $k + 1/2$ and growth rate $-\log(1 - m/p)$, viz.,

$$w_j^{k,m,p} \approx \frac{1}{1 + \left(1 - \frac{m}{p}\right)^{k-j+1/2}}. \quad (6)$$

This indicates that, in contrast to FS, for the same weight budget k , RGS distributes its weights across a larger number of features through a smoothing filter enabled by the controlled randomization.

We state these facts more rigorously and discuss them further in Section 4, with all proofs deferred to the supplement [16]. For now, we note that since FS is equivalent to RGS if we set $m = p$, varying k and m in (6) carves out a more flexible family of solutions compared to FS. We will show that fixing k and optimizing over m has the potential to yield both a better fit (via training error) as well as better regularization (via degrees of freedom).

3.3 Degrees of Freedom Improvement

We first show that under a reasonable assumption, decreasing the feature subsampling parameter m (i.e., decreasing the subsampling ratio) has the effect of decreasing the degrees of freedom of the model.

Theorem 3.1. *Grant Assumption 3.1 and suppose $k \mapsto \text{df}(\hat{f}_{k,p})$ forms a concave sequence.⁵ Let $m < m'$. Then, for all $k, p \geq 1$, we have*

$$\text{df}(\hat{f}_{k,m,p}) \leq \text{df}(\hat{f}_{k,m',p}).$$

In particular, $k \leq \text{df}(\hat{f}_{k,m,p}) \leq \text{df}(\hat{f}_{k,p})$ for all m .

This result stems from the fact that under Assumption 3.1, the RGS estimator $\hat{f}_{k,m,p}$ can be written as a convex combination of the FS estimators for different values of k , while the degrees of freedom operator is linear in its input. The core technical tool is a coupling-based construction of the RGS process, in which estimators at different subsampling levels m are defined on a shared probability space using the same underlying randomness. This allows us to directly compare their induced weight vectors $w_j^{k,m,p}$ and establish that they form a majorization hierarchy indexed by m .⁶ The linearity of the degrees of freedom also allows us to argue that the concavity condition on the degrees of freedom of FS in Theorem 3.1 is likely to hold in low SNR scenarios, in particular, when $|\hat{\beta}_{k,p}| \gg |\beta_{k,p}|$. Indeed, in such a scenario, we have

$$\begin{aligned} \frac{\sigma^2}{n} \left(\text{df}(\hat{f}_{k,p}) - \text{df}(\hat{f}_{k-1,p}) \right) &= \frac{\sigma^2}{n} \text{df} \left(\hat{\beta}_{k,p} x_{k,p} \right) \\ &= \mathbb{E} \left[\hat{\beta}_{k,p} \left(\hat{\beta}_{k,p} - \beta_{k,p} \right) \right] \\ &\approx \mathbb{E} \left[\hat{\beta}_{k,p}^2 \right], \end{aligned} \tag{7}$$

which is a non-increasing sequence in k according to Definition 3.1. Empirical support for the degrees of freedom of FS being concave with respect to k , even in non-orthogonal settings, can be found in Figures 1 and 4 of [33] and Figure 7 of [43].

Remark. For a constant model (i.e., $\beta = \mathbf{0}$), the approximation in (7) becomes exact.

3.4 Expected Training Error Improvement

Because of the previous section, one can roughly interpret the act of varying m as reallocating the weight/parameter budget of the RGS model among the different features. We now state a lower bound for the reduction in training error attainable from this reallocation. In what follows, we let \hat{m} be the value of m that minimizes the training error $\|\mathbf{y} - \hat{\mathbf{f}}_{k,m,p}\|^2$.

Theorem 3.2 (Training Error Improvement). *Grant Assumption 3.1 and fix $k \geq 1$. Assume p is large enough so that $p \geq C \left(\frac{\sum_{j=1}^k \mathbb{E}[\hat{\beta}_{j,p}^2]}{\sum_{j=k+1}^{2k} \mathbb{E}[\hat{\beta}_{j,p}^2]} \right)^3$, where C is a positive constant that depends*

⁵A sequence c_1, c_2, \dots, c_p is concave if its first difference sequence $c_2 - c_1, c_3 - c_2, \dots, c_p - c_{p-1}$ is decreasing.

⁶Formally, for $m < m'$,

$$\sum_{j=1}^l w_j^{k,m,p} \leq \sum_{j=1}^l w_j^{k,m',p} \quad \text{for all } l = 1, \dots, p,$$

with equality when $l = p$.

only on k . Then,

$$\mathbb{E}[\|\mathbf{y} - \hat{\mathbf{f}}_{k,\hat{m},p}\|^2] \leq \mathbb{E}[\|\mathbf{y} - \hat{\mathbf{f}}_{k,p}\|^2] - \frac{1}{4} \frac{\left(\frac{1}{k} \sum_{j=k+1}^{2k} \mathbb{E}[\hat{\beta}_{j,p}^2]\right)^2}{\frac{1}{k} \sum_{j=1}^k \mathbb{E}[\hat{\beta}_{j,p}^2]}. \quad (8)$$

Note that the performance gap in (8) is larger when the coefficients $\hat{\beta}_{k+1,p}, \hat{\beta}_{k+2,p}, \dots$ corresponding to features omitted by FS has a slower rate of decay. This makes intuitive sense, because in such a setting, allocating the weight budget more evenly across more features can lead to a better fit.

4 Properties of RGS Weights and Coefficients

In this section, we further analyze the RGS weights $w_j^{k,m,p}$ under Assumption 3.1. We first note that the weights are non-increasing. That is, for all $j < j'$ and $k, m, p \geq 1$, one can show that $w_j^{k,m,p} \geq w_{j'}^{k,m,p}$. In addition, we have the following recurrence relation, which will be our main technical tool.

Lemma 4.1 (Recurrence Relation). *The weights satisfy the recurrence relation*

$$w_j^{k,m,p} = \frac{\binom{p-j}{m-1}}{\binom{p}{m}} + \frac{\binom{p-j}{m}}{\binom{p}{m}} w_j^{k-1,m,p-1} + \left(1 - \frac{\binom{p-j+1}{m}}{\binom{p}{m}}\right) w_{j-1}^{k-1,m,p-1}, \quad (9)$$

where $w_j^{0,m,p} = w_j^{k,m,0} = w_0^{k,m,p} = 0$.

4.1 Logistic Approximation

The recurrence (9) is three-dimensional (in j , k , and p) and non-homogeneous, making it highly challenging to find a simple closed-form solution. However, in the scaling limit as $m \rightarrow \infty$, $p \rightarrow \infty$, and $m/p \rightarrow \gamma$ for some constant $\gamma \in [0, 1]$, the recurrence converges to a two-dimensional system that decouples into a one-dimensional subsystem with an explicit analytical solution.⁷ This yields the following theorem.

Theorem 4.1 (Asymptotic Weights for Fixed k). *The limiting weights $\tilde{w}_j^{k,\gamma} := \lim_{\substack{m \rightarrow \infty, p \rightarrow \infty \\ m/p \rightarrow \gamma}} w_j^{k,m,p}$*

(a) *exist and equal*

$$\sum_{i=1}^k (-1)^{k-i} \prod_{l=i}^k \left(e^{-\alpha(j-l)} - e^{-\alpha j}\right), \quad (10)$$

(b) *satisfy the bounds*

$$\frac{1}{1 + e^{-\alpha(h(\alpha,k)-j)}} \leq \tilde{w}_j^{k,\gamma} \leq \frac{1}{1 + e^{-\alpha(h(\alpha,k)+1-j)}}, \quad (11)$$

where $h(\alpha, k) := \frac{1}{\alpha} \log(e^{\alpha k} - 1)$ and $\alpha \in (0, \infty)$ is defined via $\gamma = 1 - e^{-\alpha}$.

⁷Note that it is standard practice to take $m = \lfloor p/3 \rfloor$ in RFs, which corresponds to $\gamma = 1/3$.

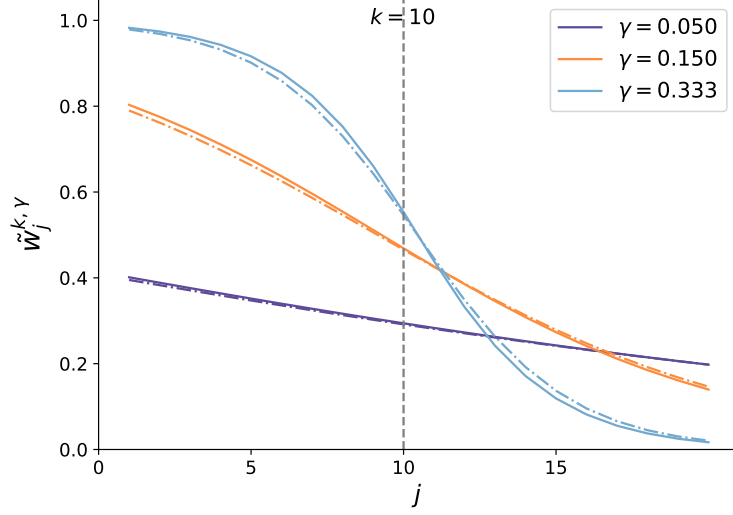


Figure 2: Comparison of $\tilde{w}_j^{k,\gamma}$ (solid) and the logistic approximation (6) (dashed) for $\gamma = 0.05, 0.15,$ and $0.333,$ with $k = 10.$

The statement in (11) reveals that the weights are sandwiched between two logistic functions with midpoints $h(\alpha, k)$ and $h(\alpha, k) + 1$ and growth rate $\alpha = -\log(1 - \gamma)$. Moreover, when αk is large, $h(\alpha, k) \approx k$, and when γ is small, $\alpha \approx \gamma$, which reveals how the RGS parameters directly affect the shape of its weight function.⁸ Specifically, as k increases, the function gets translated towards the right; as γ increases (corresponding to larger m), the function becomes more compressed around its midpoint and thereby more closely approximates the sharp thresholding behavior of FS. Figure 2 illustrates this behavior by plotting $\tilde{w}_j^{k,\gamma}$ for three values of γ : 0.05, 0.15, and 0.333.

Interestingly, the approximation of the weights by a logistic function becomes more exact, differing only in a half-index shift as opposed to a full-index shift, if we also let the selection threshold k tend to infinity. In the following theorem, we introduce a new parameter $d = k - j$, which represents the “offset” from the selection threshold.

Theorem 4.2 (Asymptotic Weights for Large k). *The limiting weights $\check{w}_d^\gamma := \lim_{k \rightarrow \infty} \lim_{\substack{m \rightarrow \infty, p \rightarrow \infty \\ m/p \rightarrow \gamma}} w_{k-d}^{k,m,p}$*

(a) *exist and equal*

$$\sum_{i=0}^{\infty} (-1)^i e^{-\alpha i(d+i/2+1/2)}, \quad (12)$$

(b) *satisfy the symmetry property $\check{w}_d^\gamma = 1 - \check{w}_{-(d+1)}^\gamma$,*

(c) *satisfy the bounds*

$$(i) \quad \frac{1}{1+e^{-\alpha d}} \leq \check{w}_d^\gamma \leq \frac{1}{1+e^{-\alpha(d+1/2)}}, \quad d < 0,$$

⁸In fact, if the sampling of the features in RGS is performed *with* replacement, then all asymptotic results hold with α replaced by γ .

$$(ii) \frac{1}{1+e^{-\alpha(d+1/2)}} \leq \check{w}_d^\gamma \leq \frac{1}{1+e^{-\alpha(d+1)}}, \quad d \geq 0,$$

(d) have a sigmoidal (e.g., S-shaped) pattern with respect to d .⁹

Observe that properties (b) and (d) in Theorem 4.2 both also apply to the logistic function. Finally, since $w_j^{k,m,p} \approx \check{w}_{k-j}^\gamma$ and $\gamma = 1 - e^{-\alpha} \approx m/p$ for large k , m , and p , the refined logistic bounds in part (c) of Theorem 4.2 imply the approximation formula we stated earlier as (6).

4.2 Comparisons with Elastic Net

It is instructive to compare the behavior of RGS with that of elastic net regression. Introduced in [63], elastic net is a popular method that combines the ℓ_1 and ℓ_2 penalties of lasso and ridge regression, respectively. Specifically, it solves the convex optimization problem

$$\hat{\beta}^{\text{EN}} = \arg \min_{\beta \in \mathbb{R}^p} \left\{ \|\mathbf{y} - \mathbf{X}\beta\|^2 + \lambda_1 \|\beta\|_{\ell_1} + \lambda_2 \|\beta\|_{\ell_2}^2 \right\},$$

where λ_1 and λ_2 are non-negative tuning hyperparameters. Under Assumption 3.1, the elastic net estimator takes a particularly simple form. As shown in [63], the elastic net coefficient for $x_{j,p}$ can be expressed as

$$\hat{\beta}_{j,p}^{\text{EN}} = \frac{(|\hat{\beta}_{j,p}| - n\lambda_1/2)_+}{1 + n\lambda_2} \text{sgn}(\hat{\beta}_{j,p}), \quad (13)$$

where $\hat{\beta}_{j,p}$ is the ordered OLS coefficient from Definition 3.1. For comparison, using the representation (5) and approximation (6), the RGS coefficient for $x_{j,p}$ has the form:

$$\hat{\beta}_{j,p}^{\text{RGS}} \approx \frac{\hat{\beta}_{j,p}}{1 + \left(1 - \frac{m}{p}\right)^{k-j+1/2}}.$$

Elastic net was originally designed to relax lasso's preference for highly sparse solutions, which was observed to create instability when features are highly correlated. From (13), we see that it has the same effect even in an orthogonal setting. Since all non-zero coefficients are shrunk by a constant factor of $1/(1 + n\lambda_2)$, the parameter budget of the model can be spread out across more coefficients. While this is somewhat similar in spirit to the role of the feature subsampling in RGS, the family of solutions attainable using both strategies is different, thereby yielding different predictive performances on any given dataset.

4.3 Revisiting Best Subset vs Lasso

In the sparse linear regression literature, Hastie, Tibshirani, and Tibshirani [33] compared BSS and lasso, showing via numerical experiments that in high-SNR settings, BSS (and FS)

⁹This means that

- (i) $\check{w}_d^\gamma \leq \check{w}_{d+1}^\gamma, \quad d \in \mathbb{Z}$,
- (ii) $\check{w}_d^\gamma - \check{w}_{d-1}^\gamma \leq \check{w}_{d+1}^\gamma - \check{w}_d^\gamma, \quad d < 0$,
- (iii) $\check{w}_d^\gamma - \check{w}_{d-1}^\gamma \geq \check{w}_{d+1}^\gamma - \check{w}_d^\gamma, \quad d \geq 0$.

seem to have higher accuracy than lasso. In contrast, in low-SNR regimes, they showed that lasso outperforms BSS.¹⁰ They explain this by observing that “different procedures bring us from the high-bias to the high-variance ends of the tradeoff along different model paths”, with the solution path of neither algorithm completely dominating the other. Our weight calculations, together with our earlier theoretical results, adds to their discussion by showing that the BSS solution path is not Pareto optimal. The RGS weights also offer an alternative solution path to those traversed by lasso and elastic net, thereby revealing how these may potentially have limitations.

4.4 Shrinkage

While decreasing the feature subsampling parameter m does not necessarily shrink each coefficient in the RGS solution (since some weights increase while others decrease), it does have the effect of shrinking the fitted values towards zero. We state this fact in terms of the following theorem, whose proof relies on establishing that the RGS weight sequences define a majorization hierarchy parameterized by m .

Theorem 4.3. *Grant Assumption 3.1 and let $m < m'$. Then, for any $k, p \geq 1$, we have*

$$\|\hat{\mathbf{f}}_{k,m,p}\| \leq \|\hat{\mathbf{f}}_{k,m',p}\|.$$

Evidently, the largest shrinkage occurs when $m = 1$, in which case $\|\hat{\mathbf{f}}_{k,1,p}\| = \sqrt{k/p}\|\hat{\boldsymbol{\beta}}\|_{\ell_2}$, and the smallest shrinkage occurs when $m = p$, in which case RGS becomes FS.

5 Numerical Experiments

In this section, we describe the results of several numerical experiments that illustrate the predictive effectiveness of RGS vis-à-vis other sparse regression methods. Furthermore, our experiments provide evidence that our theoretical results generalize beyond the idealized assumptions, such as orthogonal features, required in Section 3. We present only the key settings and findings, with additional experiments found in the supplement.

5.1 Experimental Design

5.1.1 Data Generating Process

We generate i.i.d. training data $\{(\mathbf{x}_i, y_i)\}_{i=1}^n$, where $\mathbf{x}_i \in \mathbb{R}^p$ has the distribution $\mathbf{x}_i \sim \mathcal{N}(\mathbf{0}, \boldsymbol{\Sigma})$, $y_i = \boldsymbol{\beta}^\top \mathbf{x}_i + \varepsilon_i$, with $\varepsilon_i \sim \mathcal{N}(0, \sigma^2)$, independent of \mathbf{x}_i . Following Hastie et al. [33], we investigate two covariance structures: (i) *banded correlation*, in which the (i, j) entry of $\boldsymbol{\Sigma}$ satisfies $\Sigma_{ij} = \rho^{|i-j|}$, and (ii) *block correlation*, in which $\Sigma_{ii} = 1$, $\Sigma_{ij} = 0.25$ if features i and j lie in the same block, and $\Sigma_{ij} = 0$ otherwise. We investigate two types of regression vectors: (i) *exact sparsity*, whereby $\beta_i = 1$ for $1 \leq i \leq s$ and $\beta_i = 0$ otherwise, and (ii) *inexact sparsity*, whereby $\beta_i = 1$ for $1 \leq i \leq s$ and $\beta_i = (-1)^i \exp(-i/2)$ for

¹⁰See [30] for some recent theoretical work supporting this observation.

$s < i \leq p$. Note that here we use a fixed ordering of the features instead of the data-dependent ordering used in our theoretical discussions. We fix $n = 1000$, $s = 10$, and vary $p \in \{100, 200, 400, 500, 800\}$, $\rho \in \{0.10, 0.25, 0.50, 0.75\}$. Furthermore, we vary σ^2 so that the signal-to-noise ratio (SNR), defined as $\text{SNR} := \mathbb{E}[(\boldsymbol{\beta}^\top \mathbf{x})^2]/\sigma^2 = \boldsymbol{\beta}^\top \boldsymbol{\Sigma} \boldsymbol{\beta}/\sigma^2$, lies in the grid $\{0.031, 0.053, 0.11, 0.25, 1.0\}$. These values correspond to a roughly geometric grid $\{0.03, 0.05, 0.1, 0.2, 0.5\}$ under the normalized scaling $\text{SNR}/(\text{SNR} + 1)$.¹¹

5.1.2 Methods and Hyperparameters

We compare RGS against GS (FS) as well as two other randomized ensembling methods for GS: (i) bagging [7] and (ii) smearing [9]. We also compare against lasso regression [51] and elastic net [63], which are two of the most commonly used convex relaxation methods for sparse regression. We optimized the hyperparameters for all the methods based on 10-fold cross validation. We varied the hyperparameters (k, m) for RGS by considering every $k \in [20]$ and $m \in \{[2 + (p - 2)(1.5^i - 1)/(1.5^9 - 1)]_{i=0}^9\}$. This formula for m was chosen to consider values growing exponentially, with more values considered near 1 than p , as standard literature on random forests suggest that lower values of m , particularly $m = 1/3$, are closer to the optimum. The number of base learners in each ensembling method was set at $B = 500$.

5.1.3 Evaluation Metrics

We evaluated the performance of each method according to two metrics: (i) the *relative in-sample error* (RISE), defined as $\|\hat{\boldsymbol{\beta}} - \boldsymbol{\beta}\|_{\hat{\boldsymbol{\Sigma}}}^2/\sigma^2 + 1$, where $\hat{\boldsymbol{\Sigma}}$ is the sample covariance $\mathbf{X}^\top \mathbf{X}/n$, and (ii) the *relative test error* (RTE), defined as $\|\hat{\boldsymbol{\beta}} - \boldsymbol{\beta}\|_{\boldsymbol{\Sigma}}^2/\sigma^2 + 1$. The RISE can be shown to be equivalent to the value $\mathbb{E}[\|\hat{\mathbf{f}} - \mathbf{y}'\|^2]/\sigma^2$, where $\hat{\mathbf{f}}$ is the vector of fitted values, and $y'_i = f(\mathbf{x}_i) + \varepsilon'_i$, with $\varepsilon'_i \sim \mathcal{N}(0, \sigma^2)$ drawn independently of the training data. It hence measures the ratio of the in-sample error to the Bayes error. Similarly, the RTE can be shown to be equivalent to $\mathbb{E}_{(\mathbf{x}, y)}[(\hat{\boldsymbol{\beta}}^\top \mathbf{x} - y)^2]/\sigma^2$, where (\mathbf{x}, y) is a fresh example drawn from the same distribution as the training set. This is hence the ratio of the test error to the Bayes error. We include both metrics because while the former is more relevant to fixed design linear regression, which is the framework used in our theoretical analysis, the latter is more relevant to modern machine learning. The reported values for both metrics were computed by averaging over 10 experimental replicates.

5.2 Results

In Figure 3, we show the RISE values for all methods under exact sparsity, banded correlation with $\rho = 0.5$, and aspect ratios $p/n = 0.1, 0.8$, as SNR is varied over the full grid of values. All other results are deferred to Section B in the supplement. Similar to Hastie et al. [33], we observe that GS tends to outperform lasso at high SNR values, but suffers from poor performance at low SNR values. On other hand, RGS seems to uniformly outperform GS,

¹¹This transformed quantity is sometimes called the “perfect score” proportion of variance explained (PVE) [32, 1] and is also known as heritability in genomics [53].

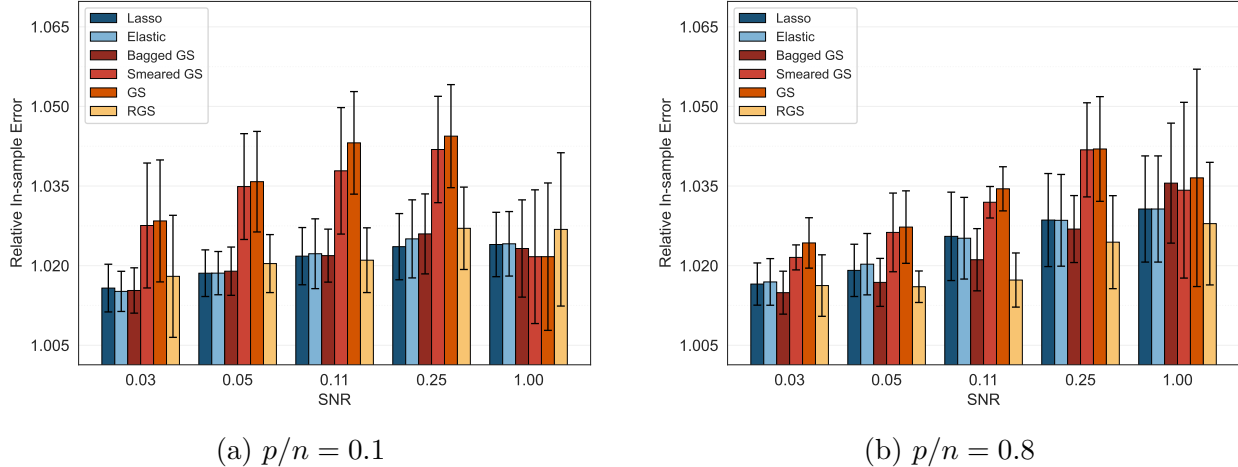


Figure 3: The relative in-sample error for various sparse regression methods across $\text{SNR} \in \{0.031, 0.053, 0.11, 0.25, 1.0\}$ for banded exact sparsity data. RGS together with bagged GS seem to uniformly outperform all other methods.

and is competitive with both lasso and elastic net at low SNR values. Furthermore, it tends to outperform smearing and has similar performance to bagging, but with much higher computational efficiency, with RGS being about 5x faster than bagging per model fit on an AMD Ryzen 7 7800X3D CPU without parallelization. Finally, the improvement of RGS over other methods seems to be larger at a higher aspect ratio. These observations are relatively robust to the choice of aspect ratio, covariance structure, sparsity structure, and the choice of evaluation metric. In additional experiments, we also found our conclusions to hold even with non-Gaussian and heavy-tailed noise.

5.3 Bias-Variance Trade-Off

Towards validating Theorem 3.1 and Theorem 3.2 under non-orthogonal designs, we computed the degrees of freedom and training error for RGS for each fixed value of k , with m selected via cross-validation, and compared them against the corresponding values for GS for the same value of k . We performed this for each simulation setting discussed in Section 5.1.1. The results for exact sparsity, banded correlated features with $\rho = 0.5$, $\text{SNR} = 0.053, 0.25, 1.0$, and $p/n = 0.1$ are shown in Figure 4. We observe that for $\text{SNR} = 0.053, 0.25$, for each model size k , using RGS over GS decreases both the degrees of freedom and training error, thereby shifting the entire bias-variance tradeoff curve towards the bottom left. The gains are more significant when SNR is lower, which is in accordance with Figure 3. On the other hand, for high SNR (such as $\text{SNR} = 1$), RGS tends to perform more poorly around $k = 10$. This phenomenon is partly explained in Proposition 6.1 to come. Additional results for other settings are deferred to Section B in the supplement.

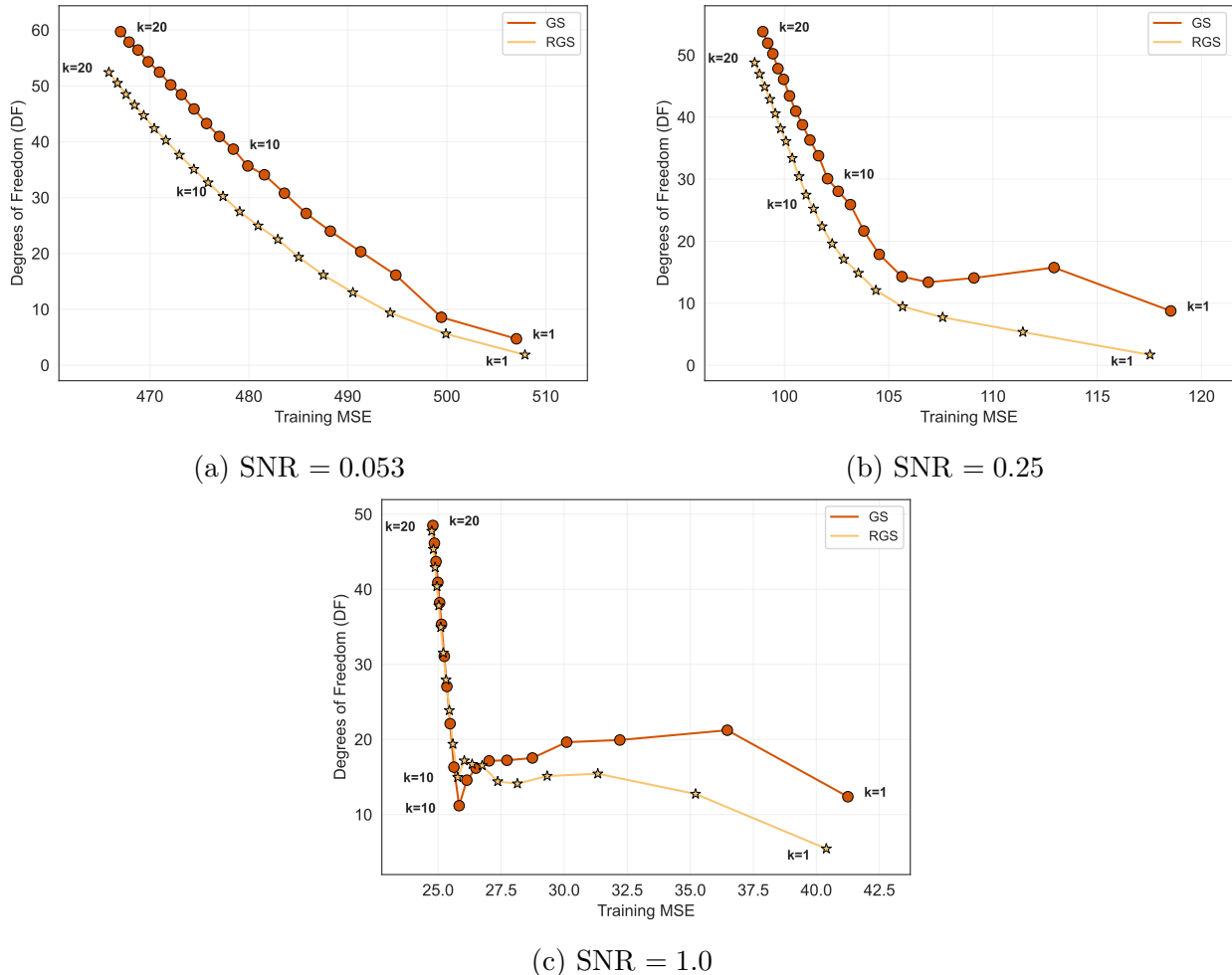


Figure 4: Degrees of freedom (y-axis) vs. training MSE (x-axis) for RGS and GS with $p/n = 0.1$, banded exact sparsity, as we vary $k \in [20]$, with the “true” value being 10. For each value of k , RGS decreases both the degrees of freedom as well as training MSE, thereby shifting the tradeoff curve towards the bottom left. The gains are more significant at low SNR. At high SNR, RGS and GS become similar.

6 Explaining the Role of Randomization in RFs

RFs [10] consist of ensembles of regression (or classification) trees, each of which recursively partitions the feature space, with each split (on a particular feature and at a particular threshold) selected by greedily optimizing a local performance criterion [11]. Each tree is randomized by bootstrapping the training dataset (bagging) and by randomly constraining the set of features that can be split on at each iteration, that is, by feature subsampling. Because of their resounding empirical success [15, 27, 45], there has been a significant amount of work on understanding the statistical and mathematical properties of RFs, such as on their consistency, convergence rates, and asymptotic normality, under various data generating scenarios [50, 42, 6, 36, 17, 2]. On the other hand, the exact role played by randomization in the effectiveness of RFs remains unclear, with there being much disagreement and debate [10,

32, 56, 43, 19, 38, 41, 49]. In this section, we summarize these developments and discuss how our results provide empirical and theoretical evidence for or against various arguments.

Breiman [10] originally explained the benefits of randomization as increasing diversity among the trees, thereby reducing the variance in their predictions. Interestingly, in his concluding remarks, he speculated that randomization may “act to reduce bias” but that “the mechanism for this is not obvious”. These two explanations have had divergent fates, with Hastie, Tibshirani, and Friedman [32] arguing in their influential textbook that “the improvements in prediction obtained by bagging or random forests are solely a result of variance reduction”.

Seminal work by Mentch and Zhou [43] elaborated on this hypothesis. They focused on the role played by feature subsampling and (i) found in their numerical experiments that decreasing the feature subsampling ratio γ decreases the degrees of freedom in RFs. To further explore the generality of this phenomenon, they considered a version of RGS that also incorporates bagging, (ii) finding that the degrees of freedom in RGS also decreases with γ . They hence (iii) concluded that feature subsampling “serves as a form of implicit regularization” and that γ “serves much the same purpose as the shrinkage penalty in explicitly regularized regression procedures like lasso and ridge regression”. Their claim was seemingly supported by a wave of theoretical work analyzing ensembles of (non-adaptive) OLS estimators randomized via feature subsampling, with the broad conclusion that the resulting estimator is mathematically equivalent to ridge regression [37, 48], in an asymptotic sense.

Our results suggest, contrary to this line of work, that the analogy between γ and λ , the shrinkage penalty in ridge or lasso regression, is more nuanced in the context of greedy, adaptive methods like RGS (and RFs). Note that in both ridge and lasso regression, the expected training error (resp. degrees of freedom) is monotonically increasing (resp. monotonically decreasing) in λ [64, 32], thereby giving an exact trade-off between the two quantities. However, this is not what happens with γ in RGS. Our Theorem 3.2 shows that the training error for RGS is not monotonic in γ and instead is minimized at an intermediate value. Meanwhile, although Theorem 3.2 in our paper gives a sufficient condition for which the degrees of freedom is monotonically decreasing in γ , which generally holds in lower SNR regimes and seems to corroborate observation (ii) above, it is easy to construct an example where this monotonicity fails in higher SNR regimes:

Proposition 6.1. *Grant Assumption 3.1 and suppose that the regression vector β is exactly s -sparse (all nonzero coefficients are equal to 1) and that the noise variables are Gaussian. Then we have*

$$\lim_{\substack{m, p, n \rightarrow \infty, \\ m/p \rightarrow \gamma}} \frac{\text{df}(\hat{f}_{k, m, p}) - \text{df}(\hat{f}_{k, p})}{\log p} \geq C,$$

where C is a constant depending only on γ and k .

The breakdown in the analogy between γ and λ can also be seen in the fitted coefficients. While the ridge or lasso coefficients shrink toward zero as λ increases, the weight formulas (Theorems 4.1 and 4.2) for RGS show that varying γ simultaneously shrinks some coefficients while inflating others. In summary, the role of feature subsampling in RGS is altogether more complex than providing shrinkage. As mentioned in previous sections, the flexibility

of being able to vary γ has the effect of enlarging the model search space, which can lead to simultaneously better model fit and lower model complexity.

While our theory applies only to RGS, it coheres with the claims of a number of very recent works that randomization in RFs can reduce “bias” [19, 38, 41, 49]. While each of these works uses a different definition of bias, all definitions become equivalent to the classical definition if, similar to our analysis of RGS, we consider RFs in the limit of infinite trees, which exists by the law of large numbers. In this case, the bias of the RF estimator \hat{f} is defined as $\mathbb{E}\left[\left(f(\mathbf{x}_0) - \mathbb{E}\left[\hat{f}(\mathbf{x}_0)\right]\right)^2\right]$, where the inner expectation is taken with respect to the training set and the outer expectation is taken with respect to a new data point \mathbf{x}_0 .

In these works, we identify two mechanisms for bias reduction. The first mechanism is by *enhancing the approximation power of RFs*. As observed Curth et al. [19], the class of decision tree models that can be fitted on a fixed dataset is not convex, so by taking simple averages of these decision trees, we enlarge the class of possible models.¹² Via numerical experiments, they showed that when varying γ while fixing all other hyperparameters, minimum bias can be achieved at intermediate value of γ . Mei et al. [41] gave an interesting theoretical argument to support this statement when the true regression function is linear.¹³ Note that this argument is entirely analogous to our explanation for how randomization in RGS improves model fit (c.f., Remark 3.1.) A second mechanism is by *overcoming potential failures of greedy optimization*, which is used by the base learners of RFs. Specifically, Liu and Mazumder [38] showed numerically how certain “hidden patterns” that would otherwise be missed can be detected upon injecting randomness into the tree-growing process, leading to smaller bias. While this mechanism has no analogy in our theoretical analysis of RGS (again c.f., the remark in Section 3.A.), it is easy to construct an example showing how it may arise in RGS as well (c.f., Example A.1 in the supplement).

Taken together, these results broaden our perspective on the role of randomization in the success of RFs. Whereas Mentch and Zhou [43] concluded that feature subsampling is mainly useful in low SNR regimes, these recent results show that it can also be useful even in the absence of any noise [19]. Furthermore, since feature subsampling is popularly viewed as a form of implicit regularization, these results urge us to pay more attention to nuance in our understanding of this phenomenon, which has become of great interest to the machine learning community [54, 44, 3, 4]. Specifically, our mental models of how regularization works in ridge and lasso regression may not map neatly onto the effects of algorithmic regularization, be it from feature subsampling, dropout, or gradient descent.

7 Discussion and Future Work

The major theoretical limitations of our work are our assumptions that the features are orthogonal. This gap is somewhat bridged by our empirical results, which show that RGS

¹²To explain further, any decision tree model fitted on a fixed dataset is constrained to have leaf values that are equal to the average response in the training set over that leaf. In particular, they cannot have empty leaves. It is easy to see that this constraint makes this class of functions non-convex.

¹³Their proof, however, relies on an oracle tree-growing process.

continues to provide performance gains even in correlated settings, such as under banded and block covariance structures. Nonetheless, a promising direction for future work is to explain these results theoretically. For example, one could study how small deviations from orthogonality (e.g., through structured perturbations of $\mathbf{X}^\top \mathbf{X}/n$) affect the RGS weights and associated bias-variance tradeoffs. Second, while we make arguments about random forests, we are only able to do so by analogy, having analyzed feature subsampling in RGS. A direct theoretical analysis of how feature subsampling improves RFs is therefore of significant interest. Partial results were obtained by Mei et al. [41], but they require certain oracle assumptions, which make their analysis deviate from how RFs are used in practice.

In addition, RGS faces certain practical limitations. While RGS significantly reduces computational complexity via our dynamic programming implementation, its efficiency gains diminish as k grows large relative to p . Investigating further computational optimizations—such as parallelized implementations or approximate search heuristics—would be beneficial for scaling to ultra-high-dimensional datasets.

By addressing these challenges, RGS has the potential to become a broadly useful tool for sparse modeling, particularly in high-stakes domains that demand both accuracy and interpretability. Promising application areas include high-dimensional causal inference and deep learning pipelines as a feature selection module.

Acknowledgements

J.M.K. was partially supported from the National Science Foundation (NSF) through CAREER DMS-2239448. Y.S.T. was supported from NUS Startup Grant A-8000448-00-00 and MOE AcRF Tier 1 Grant A-8002498-00-00.

References

- [1] Abhineet Agarwal, Ana M Kenney, Yan Shuo Tan, Tiffany M Tang, and Bin Yu. Integrating random forests and generalized linear models for improved accuracy and interpretability. *arXiv preprint arXiv:2307.01932*, 2023.
- [2] Ludovic Arnould, Claire Boyer, and Erwan Scornet. Is interpolation benign for random forest regression? In *International Conference on Artificial Intelligence and Statistics*, pages 5493–5548. PMLR, 2023.
- [3] Sanjeev Arora, Nadav Cohen, Wei Hu, and Yuping Luo. Implicit regularization in deep matrix factorization. In H. Wallach, H. Larochelle, A. Beygelzimer, F. d'Alché-Buc, E. Fox, and R. Garnett, editors, *Advances in Neural Information Processing Systems*, volume 32. Curran Associates, Inc., 2019.
- [4] Peter L. Bartlett, Philip M. Long, Gábor Lugosi, and Alexander Tsigler. Benign overfitting in linear regression. *Proceedings of the National Academy of Sciences*, 117(48):30063–30070, 2020.

- [5] E. M. L. Beale, M. G. Kendall, and D. W. Mann. The discarding of variables in multivariate analysis. *Biometrika*, 54(3-4):357–366, 12 1967.
- [6] Gérard Biau and Erwan Scornet. A random forest guided tour. *Test*, 25:197–227, 2016.
- [7] Leo Breiman. Bagging predictors. *Machine Learning*, 24(2):123–140, 1996.
- [8] Leo Breiman. Heuristics of instability and stabilization in model selection. *The annals of statistics*, 24(6):2350–2383, 1996.
- [9] Leo Breiman. Randomizing outputs to increase prediction accuracy. *Machine Learning*, 40:229–242, 2000.
- [10] Leo Breiman. Random forests. *Machine Learning*, 45(1):5–32, 2001.
- [11] Leo Breiman, Jerome Friedman, RA Olshen, and Charles J Stone. *Classification and regression trees*. Chapman and Hall/CRC, 1984.
- [12] Peter Bühlmann and Sara van de Geer. *Statistics for High-Dimensional Data: Methods, Theory and Applications*. Springer Publishing Company, Incorporated, 1st edition, 2011.
- [13] Peter Bühlmann and Bin Yu. Analyzing bagging. *The Annals of Statistics*, 30(4):927 – 961, 2002.
- [14] T. Tony Cai and Lie Wang. Orthogonal matching pursuit for sparse signal recovery with noise. *IEEE Transactions on Information Theory*, 57(7):4680–4688, 2011.
- [15] Rich Caruana and Alexandru Niculescu-Mizil. An empirical comparison of supervised learning algorithms. In *Proceedings of the 23rd International Conference on Machine Learning*, pages 161–168, 2006.
- [16] Xin Chen, Jason M Klusowski, Yan Shuo Tan, and Chang Yu. Supplement to “Revisiting Randomization in Greedy Model Search”. 2025.
- [17] Chien-Ming Chi, Patrick Vossler, Yingying Fan, and Jinchi Lv. Asymptotic properties of high-dimensional random forests. *The Annals of Statistics*, 50(6):3415 – 3438, 2022.
- [18] Gwynneth H. Coogan and Ken Ono. A q-series identity and the arithmetic of hurwitz zeta functions. *Proceedings of the American Mathematical Society*, 131(3):719–724, 2003.
- [19] Alicia Curth, Alan Jeffares, and Mihaela van der Schaar. Why do random forests work? understanding tree ensembles as self-regularizing adaptive smoothers. *arXiv preprint arXiv:2402.01502*, 2024.
- [20] Geoffrey M Davis, Stephane G Mallat, and Zhifeng Zhang. Adaptive time-frequency decompositions with matching pursuit. In *Wavelet Applications*, volume 2242, pages 402–413. SPIE, 1994.
- [21] David L. Donoho and Iain M. Johnstone and. Adapting to unknown smoothness via wavelet shrinkage. *Journal of the American Statistical Association*, 90(432):1200–1224, 1995.

- [22] N.R. Draper and H. Smith. *Applied Regression Analysis*. Applied Regression Analysis. Wiley, 1966.
- [23] Jin-Hong Du, Pratik Patil, and Arun Kumar Kuchibhotla. Subsample ridge ensembles: Equivalences and generalized cross-validation. *arXiv preprint arXiv:2304.13016*, 2023.
- [24] Bradley Efron, Trevor Hastie, Iain Johnstone, and Robert Tibshirani. Least angle regression. *The Annals of Statistics*, 32(2):407 – 499, 2004.
- [25] S. Elaydi. *An Introduction to Difference Equations*. Undergraduate Texts in Mathematics. Springer New York, 2005.
- [26] Jianqing Fan and Runze Li. Variable selection via nonconcave penalized likelihood and its oracle properties. *Journal of the American statistical Association*, 96(456):1348–1360, 2001.
- [27] Manuel Fernández-Delgado, Eva Cernadas, Senén Barro, and Dinani Amorim. Do we need hundreds of classifiers to solve real world classification problems? *The Journal of Machine Learning Research*, 15(1):3133–3181, 2014.
- [28] Luqin Gan and Genevera I Allen. Fast and interpretable consensus clustering via minipatch learning. *PLOS Computational Biology*, 18(10):e1010577, 2022.
- [29] Luqin Gan, Lili Zheng, and Genevera I Allen. Model-agnostic confidence intervals for feature importance: A fast and powerful approach using minipatch ensembles. *arXiv preprint arXiv:2206.02088*, 2022.
- [30] Shubhangi Ghosh, Yilin Guo, Haolei Weng, and Arian Maleki. Signal-to-noise ratio aware minimax analysis of sparse linear regression. *arXiv preprint arXiv:2501.13323*, 2025.
- [31] GH Hardy, JE Littlewood, and G Pólya. *Inequalities*. Cambridge University Press, 1988.
- [32] Trevor Hastie, Robert Tibshirani, Jerome H Friedman, and Jerome H Friedman. *The Elements of Statistical Learning: Data Mining, Inference, and Prediction*, volume 2. Springer, 2009.
- [33] Trevor Hastie, Robert Tibshirani, and Ryan Tibshirani. Best subset, forward stepwise or lasso? analysis and recommendations based on extensive comparisons. *Statistical Science*, 35(4):579–592, 11 2020.
- [34] Trevor Hastie, Robert Tibshirani, and Martin Wainwright. Statistical learning with sparsity. *Monographs on statistics and applied probability*, 143(143):8, 2015.
- [35] Ronald R Hocking and RN Leslie. Selection of the best subset in regression analysis. *Technometrics*, 9(4):531–540, 1967.
- [36] Jason Klusowski. Sharp analysis of a simple model for random forests. In *International Conference on Artificial Intelligence and Statistics*, pages 757–765. PMLR, 2021.

- [37] Daniel LeJeune, Hamid Javadi, and Richard Baraniuk. The implicit regularization of ordinary least squares ensembles. In *International Conference on Artificial Intelligence and Statistics*, pages 3525–3535. PMLR, 2020.
- [38] Brian Liu and Rahul Mazumder. Randomization can reduce both bias and variance: A case study in random forests. *arXiv preprint arXiv:2402.12668*, 2024.
- [39] Albert W. Marshall, Ingram Olkin, and Barry C. Arnold. *Inequalities: Theory of Majorization and its Applications*, volume 143. Springer, second edition, 2011.
- [40] Rahul Mazumder and Haoyue Wang. On the convergence of CART under sufficient impurity decrease condition. *Advances in Neural Information Processing Systems*, 36, 2024.
- [41] Tianxing Mei, Yingying Fan, and Jinchi Lv. Exogenous randomness empowering random forests. *arXiv preprint arXiv:2411.07554*, 2024.
- [42] Lucas Mentch and Giles Hooker. Quantifying uncertainty in random forests via confidence intervals and hypothesis tests. *Journal of Machine Learning Research*, 17(26):1–41, 2016.
- [43] Lucas Mentch and Siyu Zhou. Randomization as regularization: A degrees of freedom explanation for random forest success. *Journal of Machine Learning Research*, 21(171):1–36, 2020.
- [44] Behnam Neyshabur, Ryota Tomioka, and Nathan Srebro. In search of the real inductive bias: On the role of implicit regularization in deep learning, 2015.
- [45] Randal S Olson, William La Cava, Zairah Mustahsan, Akshay Varik, and Jason H Moore. Data-driven advice for applying machine learning to bioinformatics problems. In *Biocomputing 2018: Proceedings of the Pacific Symposium*, pages 192–203. World Scientific, 2018.
- [46] Pratik Patil and Jin-Hong Du. Generalized equivalences between subsampling and ridge regularization. In A. Oh, T. Naumann, A. Globerson, K. Saenko, M. Hardt, and S. Levine, editors, *Advances in Neural Information Processing Systems*, volume 36, pages 78926–78963. Curran Associates, Inc., 2023.
- [47] Pratik Patil, Jin-Hong Du, and Arun Kumar Kuchibhotla. Bagging in overparameterized learning: Risk characterization and risk monotonicity. *Journal of Machine Learning Research*, 24(319):1–113, 2023.
- [48] Pratik Patil and Daniel LeJeune. Asymptotically free sketched ridge ensembles: Risks, cross-validation, and tuning. *arXiv preprint arXiv:2310.04357*, 2023.
- [49] Christos Revelas, Otilia Boldea, and Bas JM Werker. When do random forests work? *arXiv preprint arXiv:2504.12860*, 2025.
- [50] Erwan Scornet, Gérard Biau, and Jean-Philippe Vert. Consistency of random forests. *Annals of Statistics*, 43(4):1716–1741, August 2015.

- [51] Robert Tibshirani. Regression shrinkage and selection via the lasso. *Journal of the Royal Statistical Society Series B: Statistical Methodology*, 58(1):267–288, 1996.
- [52] Joel A. Tropp and Anna C. Gilbert. Signal recovery from random measurements via orthogonal matching pursuit. *IEEE Transactions on Information Theory*, 53(12):4655–4666, 2007.
- [53] Peter M Visscher, William G Hill, and Naomi R Wray. Heritability in the genomics era—concepts and misconceptions. *Nature reviews genetics*, 9(4):255–266, 2008.
- [54] Stefan Wager, Sida Wang, and Percy S Liang. Dropout training as adaptive regularization. In C.J. Burges, L. Bottou, M. Welling, Z. Ghahramani, and K.Q. Weinberger, editors, *Advances in Neural Information Processing Systems*, volume 26. Curran Associates, Inc., 2013.
- [55] Martin J. Wainwright. Sharp thresholds for high-dimensional and noisy sparsity recovery using ℓ_1 -constrained quadratic programming (lasso). *IEEE Transactions on Information Theory*, 55(5):2183–2202, 2009.
- [56] Abraham J. Wyner, Matthew Olson, Justin Bleich, and David Mease. Explaining the success of adaboost and random forests as interpolating classifiers. *Journal of Machine Learning Research*, 18(48):1–33, 2017.
- [57] Tianyi Yao, Daniel LeJeune, Hamid Javadi, Richard G. Baraniuk, and Genevera I. Allen. Minipatch learning as implicit ridge-like regularization. In *2021 IEEE International Conference on Big Data and Smart Computing (BigComp)*, pages 65–68, 2021.
- [58] Tianyi Yao, Minjie Wang, and Genevera I. Allen. Fast and accurate graph learning for huge data via minipatch ensembles. *arXiv preprint 2110.12067*, 2023.
- [59] Bin Yu. Stability. *Bernoulli*, 19(4):1484 – 1500, 2013.
- [60] Haoran Zhan, Mingke Zhang, and Yingcun Xia. Ensemble projection pursuit for general nonparametric regression. *The Annals of Statistics*, 53(1):194 – 218, 2025.
- [61] Cun-Hui Zhang. Nearly unbiased variable selection under minimax concave penalty. *The Annals of Statistics*, 38(2):894 – 942, 2010.
- [62] Zhifeng Zhang. Matching pursuits with time-frequency dictionaries. *IEEE Transactions on signal processing*, 41(12):3397–3415, 1993.
- [63] Hui Zou and Trevor Hastie. Regularization and variable selection via the elastic net. *Journal of the Royal Statistical Society Series B: Statistical Methodology*, 67(2):301–320, 2005.
- [64] Hui Zou, Trevor Hastie, and Robert Tibshirani. On the “degrees of freedom” of the lasso. *The Annals of Statistics*, 35(5):2173 – 2192, 2007.

A Proofs

A.1 Proofs for Finite RGS Weights

Proof of Lemma 4.1. Let J be denote the index of the feature selected at the first step. To derive the recurrence for $w_j^{k,m,p}$, we condition on the first selected element $x_{i,p}$, i.e., condition on the event $J = i$.

1. If $i = j$, which occurs with probability $\mathbb{P}(J = j)$, the element $x_{j,p}$ is selected in the first step. As a result, $x_{j,p}$ will always be included in \mathcal{M}_k .
2. If $i \neq j$, the remaining $k - 1$ steps are equivalent to running RGS on $p - 1$ features. The coefficients are reassigned as follows:

$$\begin{aligned}\hat{\beta}_{l,p-1} &\leftarrow \hat{\beta}_{l,p} && \text{for } l < i \\ \hat{\beta}_{l,p-1} &\leftarrow \hat{\beta}_{l+1,p} && \text{for } l \geq i,\end{aligned}$$

where $l = 1, 2, \dots, p - 1$. We then consider two subcases:

- (a) If $i > j$, which occurs with probability $\mathbb{P}(J > j)$, the index j remains unchanged in the relative ranking. The weight contribution becomes $w_j^{k-1,m,p-1}$.
- (b) If $i < j$, which occurs with probability $\mathbb{P}(J < j)$, the index j is shifted to the $(j - 1)$ -th position in the new ordering. The weight contribution becomes $w_{j-1}^{k-1,m,p-1}$.

At the first step of RGS, we select the feature with the largest absolute inner product $|\hat{\beta}_{j,p}| = |\langle \mathbf{y}, \mathbf{x}_{j,p} \rangle|$ from an m -sized subset of p features. Because there are no ties in the feature rankings, this is equivalent to selecting the minimum index j in this subset. The probability of $x_{j,p}$ being selected is thus the probability that j is the minimum index in a random m -sized subset of p elements, which is $\binom{p-j}{m-1} / \binom{p}{m}$. Therefore, by the law of total probability,

$$\begin{aligned}w_j^{k,m,p} &= \mathbb{P}(J = j) + w_j^{k-1,m,p-1} \mathbb{P}(J > j) + w_{j-1}^{k-1,m,p-1} \mathbb{P}(J < j) \\ &= \frac{\binom{p-j}{m-1}}{\binom{p}{m}} + w_j^{k-1,m,p-1} \sum_{i=j+1}^p \frac{\binom{p-i}{m-1}}{\binom{p}{m}} + w_{j-1}^{k-1,m,p-1} \sum_{i=1}^{j-1} \frac{\binom{p-i}{m-1}}{\binom{p}{m}}.\end{aligned}\tag{14}$$

Now, by the hockey-stick identity from combinatorics, we can simplify the coefficients from (14):

$$\begin{aligned}\sum_{i=j+1}^p \binom{p-i}{m-1} &= \binom{p-j}{m}, \text{ and} \\ \sum_{i=1}^{j-1} \binom{p-i}{m-1} &= \binom{p}{m} - \binom{p-j+1}{m}.\end{aligned}$$

Plugging in these two expressions into (14) gives us recurrence (9).

To prove monotonicity of the weights with respect to j , recall that $w_j^{k,m,p} = \mathbb{P}(x_{j,p} \in \mathcal{M}_k)$. Here, the randomness is over the choices of the sets, $\mathcal{V} := \{\mathcal{V}_1, \mathcal{V}_2, \dots, \mathcal{V}_k\}$. Define the events

$$\mathcal{E}_1 := \{x_{j,p} \in \mathcal{M}_k, x_{j-1,p} \notin \mathcal{M}_k\},$$

and

$$\mathcal{E}_2 := \{x_{j-1,p} \in \mathcal{M}_k, x_{j,p} \notin \mathcal{M}_k\}.$$

It suffices to show that $\mathbb{P}(\mathcal{E}_1) \leq \mathbb{P}(\mathcal{E}_2)$. To show this, we will define a measure-preserving transformation $T: \mathcal{E}_1 \rightarrow \mathcal{E}_2$ with $T(\mathcal{E}_1) \subset \mathcal{E}_2$. Assuming such a transformation exists, we have

$$\mathbb{P}(\mathcal{E}_2) \geq \mathbb{P}(T(\mathcal{E}_1)) = \mathbb{P}(\mathcal{E}_1).$$

To define T , consider $\mathcal{V} \in \mathcal{E}_1$. For this random seed, there is some index $1 \leq i \leq k$ such that $x_{j,p}$ is selected at the i -th iteration. This implies that we have $x_{j-1,p} \notin \mathcal{V}_i$, otherwise, $x_{j-1,p}$ would have been selected in the i -th step instead. Furthermore, we have $x_{j,p} \notin \mathcal{V}_l$ for $l > i$. Define $T(\mathcal{V}) := \{\mathcal{V}_1, \dots, \mathcal{V}_{i-1}, \mathcal{V}'_i, \mathcal{V}'_{i+1}, \dots, \mathcal{V}'_k\}$, where $\mathcal{V}'_i = \mathcal{V}_i \cup \{x_{j-1,p}\} \setminus \{x_{j,p}\}$, and for $l > i$, $\mathcal{V}'_l = \mathcal{V}_l$ if $x_{j-1,p} \notin \mathcal{V}_l$ otherwise $\mathcal{V}'_l = \mathcal{V}_l \cup \{x_{j,p}\} \setminus \{x_{j-1,p}\}$. Denote $\mathcal{V}' := T(\mathcal{V})$ for convenience. Let $x_{j_l,p}$ and $x_{j'_l,p}$ be the features selected at the l -th step with the set of subdictionaries \mathcal{V} and \mathcal{V}' , respectively. Note that $x_{j_l,p} = x_{j'_l,p}$ for $l = 1, \dots, i-1$, since the algorithm only makes use of $\mathcal{V}_1, \dots, \mathcal{V}_{i-1}$ to select these terms. Similarly, $x_{j_l,p} = x_{j'_l,p}$ for $l = i+1, \dots, k$, because the combinatorics depend solely on the ordinal structure of the coefficients $|\hat{\beta}_{l,p}|$. Thus, $x_{j-1,p}$ in \mathcal{V}' plays the same role as $x_{j,p}$ in \mathcal{V} . For the same reason, $\mathbb{P}(\mathcal{V}) = \mathbb{P}(\mathcal{V}')$. We also see that $\mathcal{V}' \in \mathcal{E}_2$, which proves that T is well-defined and is measure-preserving. \square

A.2 Proofs for Asymptotic RGS Weights

To prove Theorem 4.1, we give several useful lemmas. The first lemma shows that for fixed j and k , we have the following existence and recurrence.

Lemma A.1. *The limit $\tilde{w}_j^{k,\gamma} = \lim_{\substack{m \rightarrow \infty, p \rightarrow \infty \\ m/p \rightarrow \gamma}} w_j^{k,m,p}$ exists and satisfies the following recurrence*

for $j \geq 1$,

$$\tilde{w}_j^{k,\gamma} = (e^\alpha - 1)e^{-\alpha j} + e^{-\alpha j} \tilde{w}_j^{k-1,\gamma} + (1 - e^{-\alpha(j-1)}) \tilde{w}_{j-1}^{k-1,\gamma}. \quad (15)$$

However, recurrence (15) contains dependencies on both $\tilde{w}_j^{k-1,\gamma}$ and $\tilde{w}_{j-1}^{k-1,\gamma}$. These dependencies make it difficult to construct a closed form and uncover properties of $\tilde{w}_j^{k,\gamma}$. Ideally, we would like recurrences involving a change in j to be separate from recurrences involving a change in k . Fortunately, recurrence (15) can be separated into the following pair of recurrences.

Lemma A.2. *From the the recurrence in Lemma A.1, we can construct the following recurrence pair for $j \geq 1$:*

$$\tilde{w}_j^{k,\gamma} = (e^{-\alpha(j-k)} - e^{-\alpha j}) (1 - \tilde{w}_j^{k-1,\gamma}), \quad \tilde{w}_j^{0,\gamma} = 0, \quad (16)$$

$$\tilde{w}_j^{k,\gamma} = 1 - e^{-\alpha k} - \left(e^{-\alpha(k-j+1)} - e^{-\alpha k} \right) \tilde{w}_{j-1}^{k,\gamma}, \quad \tilde{w}_0^{k,\gamma} = 0. \quad (17)$$

Proof of Lemma A.1. To show the limit form of the coefficients in recurrence (15), we derive the following result using basic asymptotic facts. For a fixed j , for $m, p \rightarrow \infty$ and $m/p \rightarrow \gamma$, we have

$$\frac{\binom{p-j}{m-1}}{\binom{p}{m}} = \frac{m}{p-j-m+1} \frac{\binom{p-j}{m}}{\binom{p}{m}} = \frac{m}{p-j-m+1} \prod_{i=1}^j \frac{i+p-m}{i+p} \xrightarrow{m,p \rightarrow \infty} \frac{\gamma}{1-\gamma} (1-\gamma)^j = (e^\alpha - 1)e^{-\alpha j}.$$

Applying the same method to the other coefficients in the recurrence gives us the following:

$$\begin{aligned} \frac{\binom{p-j}{m}}{\binom{p}{m}} &\xrightarrow{m,p \rightarrow \infty} e^{-\alpha j}, \text{ and} \\ \left(1 - \frac{\binom{p-j+1}{m}}{\binom{p}{m}} \right) &\xrightarrow{m,p \rightarrow \infty} \left(1 - e^{-\alpha(j-1)} \right). \end{aligned}$$

Now, we show that $\tilde{w}_j^{k,\gamma}$ is well defined via induction on k . For the base case, let $k = 1$. Note that $w_j^{0,m,p} = 0$ for all j and all p , so

$$\tilde{w}_j^{0,\gamma} = \lim_{\substack{m \rightarrow \infty, p \rightarrow \infty, \\ m/p \rightarrow \gamma}} w_j^{0,m,p} = 0.$$

Therefore, $\tilde{w}_j^{0,\gamma}$ is well defined for all j . Now suppose that $\tilde{w}_j^{k,\gamma}$ is well defined for all steps up to k and for all j . Consider step $(k+1)$. From recurrence (9), we have

$$\begin{aligned} &\lim_{\substack{m \rightarrow \infty, p \rightarrow \infty, \\ m/p \rightarrow \gamma}} w_j^{k+1,m,p} \\ &= \lim_{\substack{m \rightarrow \infty, p \rightarrow \infty, \\ m/p \rightarrow \gamma}} \left(\frac{\binom{p-j}{m-1}}{\binom{p}{m}} + \frac{\binom{p-j}{m}}{\binom{p}{m}} w_j^{k,m,p} + w_{j-1}^{k,m,p} \left(1 - \frac{\binom{p-j+1}{m}}{\binom{p}{m}} \right) \right) \\ &= (e^\alpha - 1)e^{-\alpha j} + e^{-\alpha j} \left(\lim_{\substack{m \rightarrow \infty, p \rightarrow \infty, \\ m/p \rightarrow \gamma}} w_j^{k,m,p} \right) + \left(1 - e^{-\alpha(j-1)} \right) \left(\lim_{\substack{m \rightarrow \infty, p \rightarrow \infty, \\ m/p \rightarrow \gamma}} w_{j-1}^{k,m,p} \right) \\ &= (e^\alpha - 1)e^{-\alpha j} + e^{-\alpha j} \tilde{w}_j^{k,\gamma} + \left(1 - e^{-\alpha(j-1)} \right) \tilde{w}_{j-1}^{k,\gamma}. \end{aligned}$$

Since $\tilde{w}_j^{k,\gamma}$ and $\tilde{w}_{j-1}^{k,\gamma}$ exist for all j by inductive assumption, $w_j^{k+1,\gamma}$ exists as well for all j . Therefore, by induction, we know that the limit $\tilde{w}_j^{k,\gamma}$ exists for all j, k and satisfies the recurrence in Lemma A.1. \square

Proof of Lemma A.2. We will induct on k . First, we verify that both recurrences satisfy the base case of $k = 1$. Note that from previous arguments,

$$\tilde{w}_j^{1,\gamma} = \lim_{\substack{m \rightarrow \infty, p \rightarrow \infty, \\ m/p \rightarrow \gamma}} \frac{\binom{p-j}{m-1}}{\binom{p}{m}} = (e^\alpha - 1)e^{-\alpha j}.$$

For recurrence (16), we plug in $\tilde{w}_j^{0,\gamma} = 0$ on the right hand side:

$$\tilde{w}_j^{1,\gamma} = \left(e^{-\alpha(j-1)} - e^{-\alpha j}\right) \left(1 - \tilde{w}_j^{0,\gamma}\right) = (e^\alpha - 1)e^{-\alpha j}.$$

Thus, the recurrence (16) satisfies the base case $k = 1$. Now, note that $\tilde{w}_{j-1}^{1,\gamma} = (e^\alpha - 1)e^{-\alpha(j-1)}$. Plugging in this expression into recurrence (17), we see that

$$\tilde{w}_j^{1,\gamma} = 1 - e^{-\alpha} - \left(e^{-\alpha(1-j+1)} - e^{-\alpha}\right) \tilde{w}_{j-1}^{1,\gamma} = (e^\alpha - 1)e^{-\alpha j}.$$

Thus, both recurrences satisfy the base case.

Now, for a fixed j , suppose that both recurrences are valid for steps up to k .

Consider step $(k + 1)$. We show that $\tilde{w}_j^{k+1,\gamma}$ satisfies recurrence (16) in the following way.

We start with the recurrence from Lemma A.1:

$$\tilde{w}_j^{k+1,\gamma} = (e^\alpha - 1)e^{-\alpha j} + e^{-\alpha j} \tilde{w}_j^{k,\gamma} + \left(1 - e^{-\alpha(j-1)}\right) \tilde{w}_{j-1}^{k,\gamma}.$$

Substituting $\tilde{w}_{j-1}^{k,\gamma}$ using recurrence (17) under the inductive assumption, we obtain the following result:

$$\begin{aligned} \tilde{w}_j^{k+1,\gamma} &= (e^\alpha - 1)e^{-\alpha j} + e^{-\alpha j} \tilde{w}_j^{k,\gamma} + \left(1 - e^{-\alpha(j-1)}\right) \left(\frac{1 - e^{-\alpha k} - \tilde{w}_j^{k,\gamma}}{e^{-\alpha(k-j+1)} - e^{-\alpha k}}\right) \\ &= \left(e^{-\alpha(j-k-1)} - e^{-\alpha j}\right) \left(1 - \tilde{w}_j^{k,\gamma}\right). \end{aligned}$$

Therefore, recurrence (16) is satisfied for step $(k + 1)$. Now, we prove that recurrence (17) is satisfied for step $(k + 1)$ in a similar fashion. We plug in recurrence (16) into Lemma A.1:

$$\begin{aligned} \tilde{w}_j^{k+1,\gamma} &= (e^\alpha - 1)e^{-\alpha j} + e^{-\alpha j} \left(1 - \frac{\tilde{w}_j^{k+1,\gamma}}{e^{-\alpha(j-k-1)} - e^{-\alpha j}}\right) \\ &\quad + \left(1 - e^{-\alpha(j-1)}\right) \left(\frac{e^{-\alpha(j-k-2)} - e^{-\alpha(j-1)} - \tilde{w}_{j-1}^{k+1,\gamma}}{e^{-\alpha(j-k-2)} - e^{-\alpha(j-1)}}\right). \end{aligned}$$

Rearranging terms, we obtain the following recurrence:

$$\tilde{w}_j^{k+1,\gamma} = 1 - e^{-\alpha(k+1)} - \left(e^{-\alpha(k-j+2)} - e^{-\alpha(k+1)}\right) \tilde{w}_{j-1}^{k+1,\gamma}.$$

Thus, recurrence (17) is satisfied for step $(k + 1)$. Therefore, by induction, for a fixed j , both recurrences are satisfied for all $k \in \mathbb{N}^+$. \square

Next, we prove Theorem 4.1.

Proof of Theorem 4.1. To prove property (a), note that from Lemma A.1, we have that $\tilde{w}_j^{k,\gamma}$ exists. From (16), a first-order non-homogeneous recurrence relation with feature coefficients, we directly obtain the following closed form for $\tilde{w}_j^{k,\gamma}$ [25, Equation 1.2.4]:

$$\tilde{w}_j^{k,\gamma} = \sum_{i=1}^k (-1)^{k-i} \prod_{l=i}^k \left(e^{-\alpha(j-l)} - e^{-\alpha j}\right).$$

To prove property (b), we first show the lower bound. According to Lemma A.5, we have $\tilde{w}_j^{k,\gamma} \geq \tilde{w}_j^{k-1,\gamma}$. From (16), we know

$$\begin{aligned}\tilde{w}_j^{k,\gamma} &= \left(e^{-\alpha(j-k)} - e^{-\alpha j}\right) \left(1 - \tilde{w}_j^{k-1,\gamma}\right) \\ &\geq \left(e^{-\alpha(j-k)} - e^{-\alpha j}\right) \left(1 - \tilde{w}_j^{k,\gamma}\right).\end{aligned}$$

Therefore, solving for $\tilde{w}_j^{k,\gamma}$, we have

$$\tilde{w}_j^{k,\gamma} \geq \frac{1 - e^{-\alpha k}}{1 - e^{-\alpha k} + e^{-\alpha(k-j)}}.$$

Alternatively, we can rewrite recurrence (16) as

$$\left(e^{-\alpha(j-k-1)} - e^{-\alpha j}\right) \left(1 - \tilde{w}_j^{k,\gamma}\right) = \tilde{w}_j^{k+1,\gamma} \geq \tilde{w}_j^{k,\gamma}.$$

Solving for $\tilde{w}_j^{k,\gamma}$, we have

$$\tilde{w}_j^{k,\gamma} \leq \frac{1 - e^{-\alpha k}}{1 - e^{-\alpha k} + e^{-\alpha(k-j+1)}}.$$

Finally, note that we can write

$$\begin{aligned}\frac{1 - e^{-\alpha k}}{1 - e^{-\alpha k} + e^{-\alpha(k-j)}} &= \frac{1}{1 + (1 - e^{-\alpha k})^{-1} e^{-\alpha(k-j)}} \\ &= \frac{1}{1 + (e^{\alpha k} - 1)^{-1} e^{\alpha j}} \\ &= \frac{1}{1 + e^{-\alpha(h(a,k)-j)}}.\end{aligned}\quad \square$$

Remark. We give a remark showing that the weights $\tilde{w}_j^{k,\gamma}$ satisfy the following two additional properties. The weights $\tilde{w}_j^{k,\gamma}$

(i) are non-increasing in j for any given values of k and γ , i.e., $\tilde{w}_j^{k,\gamma} \geq \tilde{w}_{j+1}^{k,\gamma}$,

(ii) have sum $\sum_{j=1}^{\infty} \tilde{w}_j^{k,\gamma} = k$.

Property (i) directly follows from Lemma 4.1 by taking $m, p \rightarrow \infty$ and $m/p \rightarrow \gamma$.

To prove property (ii), note that from (15) we have

$$\begin{aligned}\sum_{j=1}^{\infty} \tilde{w}_j^{k,\gamma} &= \sum_{j=1}^{\infty} (e^{\alpha} - 1) e^{-\alpha j} + \sum_{j=1}^{\infty} \tilde{w}_j^{k-1,\gamma} + \sum_{j=1}^{\infty} e^{-\alpha j} \tilde{w}_j^{k-1,\gamma} - \sum_{j=1}^{\infty} e^{-\alpha(j-1)} \tilde{w}_{j-1}^{k-1,\gamma} \\ &= 1 + \sum_{j=1}^{\infty} \tilde{w}_j^{k-1,\gamma} \\ &= k,\end{aligned}$$

where we use the fact that $\tilde{w}_j^{0,\gamma} = \tilde{w}_0^{k,\gamma} = 0$.

We now turn to the proof of Theorem 4.2. Before that, we present a useful lemma regarding an alternative form of $\tilde{w}_j^{k,\gamma}$.

Lemma A.3. *The asymptotic weights $\tilde{w}_j^{k,\gamma}$ can be rewritten in the following closed form*

$$\tilde{w}_j^{k,\gamma} = \sum_{i=1}^k (-1)^{i+1} e^{\alpha i((k-j)-i/2+1/2)} \prod_{l=k-i+1}^k (1 - e^{-l\alpha}).$$

Proof of Lemma A.3. Using the closed form from (10), we re-index the sum to obtain

$$\begin{aligned} \tilde{w}_j^{k,\gamma} &= \sum_{i=1}^k (-1)^{k-i} \prod_{l=i}^k (e^{-\alpha(j-l)} - e^{-\alpha j}) \\ &= \sum_{i=0}^{k-1} (-1)^{k-i+1} e^{-(k-i)j\alpha} \prod_{l=i+1}^k (e^{l\alpha} - 1). \end{aligned}$$

Now, we note that

$$\prod_{l=i+1}^k (e^{l\alpha} - 1) = e^{\alpha(\frac{k(k+1)}{2} - \frac{i(i+1)}{2})} \prod_{l=i+1}^k (1 - e^{-l\alpha}).$$

Substituting this expression back into $\tilde{w}_j^{k,\gamma}$, we have

$$\begin{aligned} \tilde{w}_j^{k,\gamma} &= \sum_{i=0}^{k-1} (-1)^{k-i+1} e^{-(k-i)j\alpha + \alpha(\frac{k(k+1)}{2} - \frac{i(i+1)}{2})} \prod_{l=i+1}^k (1 - e^{-l\alpha}) \\ &= \sum_{i=0}^{k-1} (-1)^{k-i+1} e^{\alpha(k-i)(k-j - \frac{k-i}{2} + \frac{1}{2})} \prod_{l=i+1}^k (1 - e^{-l\alpha}). \end{aligned}$$

Finally, we re-index by setting i to be $k - i$, yielding

$$\tilde{w}_j^{k,\gamma} = \sum_{i=1}^k (-1)^{i+1} e^{\alpha i((k-j)-i/2+1/2)} \prod_{l=k-i+1}^k (1 - e^{-l\alpha}). \quad \square$$

We start to prove Theorem 4.2. For the following proofs, we perform the substitution $d = k - j$.

Proof of Theorem 4.2. To prove property (a), we first prove the existence and derive a closed form for \check{w}_d^γ slightly different from (12).

Lemma A.4. *The limit $\check{w}_d^\gamma = \lim_{\substack{k \rightarrow \infty, j \rightarrow \infty, \\ k-j=d}} \tilde{w}_j^{k,\gamma}$ exists and has the following closed form*

$$\check{w}_d^\gamma = \sum_{i=1}^{\infty} (-1)^{i+1} e^{\alpha i(d-i/2+1/2)}. \quad (18)$$

Proof of Lemma A.4. We begin by demonstrating the existence of the limit. To establish this, we first present a simple lemma regarding the monotonicity relation.

Lemma A.5. *For any given values of j and γ , we have $\tilde{w}_j^{k,\gamma} \leq \tilde{w}_j^{k+1,\gamma}$ for all $k \geq 0$.*

Proof of Lemma A.5. The proof follows directly from the following inequality:

$$\tilde{w}_j^{k,\gamma} = \lim_{\substack{m \rightarrow \infty, p \rightarrow \infty \\ m/p \rightarrow \gamma}} \mathbb{P}(x_{j,p} \in \mathcal{M}_k) \leq \lim_{\substack{m \rightarrow \infty, p \rightarrow \infty \\ m/p \rightarrow \gamma}} \mathbb{P}(x_{j,p} \in \mathcal{M}_{k+1}) = w_j(k+1, \gamma). \quad \square$$

Note that by substituting (16) into (17), we have

$$\begin{aligned} \tilde{w}_{j+1}^{k,\gamma} &= 1 - e^{-\alpha k} - e^{-\alpha(k-j)} \left(e^{-\alpha(j-k)} - e^{-\alpha j} \right) \left(1 - \tilde{w}_j^{k-1,\gamma} \right) + e^{-\alpha k} \tilde{w}_j^{k,\gamma} \\ &= e^{-\alpha k} w_j(k, \gamma) + \left(1 - e^{-\alpha k} \right) \tilde{w}_j^{k-1,\gamma}. \end{aligned}$$

Thus, $\tilde{w}_{j+1}^{k,\gamma} - \tilde{w}_j^{k-1,\gamma} = e^{-\alpha k} \left(\tilde{w}_j^{k,\gamma} - \tilde{w}_j^{k-1,\gamma} \right) \geq 0$ for all $j, k \geq 1$, where we use Lemma A.5. Fix d , let $j = k - d$, and consider the sequence $\left\{ \tilde{w}_{k-d}^{k,\gamma} \right\}_{k=d+1}^{\infty}$. This sequence is bounded and non-decreasing; thus, by the monotone convergence theorem, the limit of $\left\{ \tilde{w}_{k-d}^{k,\gamma} \right\}_{k=d+1}^{\infty}$ exists. Hence, \tilde{w}_d^γ exists and we must now identify its limit.

We will prove the closed form (18) by showing that for every $\epsilon > 0$, there exists some K such that for all $k > K$,

$$\left| \tilde{w}_{k-d}^{k,\gamma} - \sum_{i=1}^k (-1)^{i+1} e^{\alpha i(d-i/2+1/2)} \right| < \epsilon.$$

First, fix ϵ and suppose k is even. We begin by using the triangle inequality, substituting in the closed form for $\tilde{w}_{k-d}^{k,\gamma}$ we obtained in Lemma A.3:

$$\begin{aligned} & \left| \tilde{w}_{k-d}^{k,\gamma} - \sum_{i=1}^k (-1)^{i+1} e^{\alpha i(d-i/2+1/2)} \right| \\ &= \left| \sum_{i=1}^k (-1)^{i+1} e^{\alpha i(d-i/2+1/2)} \prod_{l=k-i+1}^k (1 - e^{-l\alpha}) - \sum_{i=1}^k (-1)^{i+1} e^{\alpha i(d-i/2+1/2)} \right| \\ &\leq \sum_{i=k/2+1}^k e^{\alpha i(d-i/2+1/2)} \left(1 - \prod_{l=k-i+1}^k (1 - e^{-l\alpha}) \right) + \sum_{i=1}^{k/2} e^{\alpha i(d-i/2+1/2)} \left(1 - \prod_{l=k-i+1}^k (1 - e^{-l\alpha}) \right). \end{aligned} \tag{19}$$

Suppose that $k > 2d$. We bound the first sum of (19). By basic inequalities, we have

$$\sum_{i=k/2+1}^k e^{\alpha i(d-i/2+1/2)} \left(1 - \prod_{l=k-i+1}^k (1 - e^{-l\alpha}) \right) \leq \sum_{i=k/2+1}^k e^{\alpha i(d-i/2+1/2)} \leq \frac{k}{2} \cdot e^{\alpha(k/2)(d-k/4+1/2)}.$$

When $k \rightarrow \infty$, this final expression will go 0, so there exists some K_1 such that for all $k > K_1$, the final expression is less than $\epsilon/2$.

We perform a similar computation to bound the second sum in expression (19). Note that

$$\prod_{l=k-i+1}^k (1 - e^{-l\alpha}) \geq (1 - e^{-(k-i+1)\alpha})^i \geq (1 - e^{-(k/2+1)\alpha})^{k/2}.$$

Thus,

$$1 - \prod_{l=k-i+1}^k (1 - e^{-l\alpha}) \leq 1 - (1 - e^{-(k/2+1)\alpha})^{k/2} \leq \frac{k}{2} \cdot e^{-(k/2+1)\alpha}. \quad (20)$$

Substituting expression (20) back into the second sum of expression (19), we have that

$$\begin{aligned} \sum_{i=1}^{k/2} e^{\alpha i(d-i/2+1/2)} \left(1 - \prod_{l=k-i+1}^k (1 - e^{-l\alpha}) \right) &\leq \frac{k}{2} \sum_{i=1}^{k/2} e^{\alpha i(d-i/2+1/2)} e^{-(k/2+1)\alpha} \\ &\leq \frac{k}{2} \cdot \frac{k}{2} \cdot e^{\alpha d(d-d/2+1/2)} e^{-(k/2+1)\alpha}. \end{aligned}$$

Note that as $k \rightarrow \infty$, this final expression goes to 0, so there exists some K_2 such that for all $k > K_2$, this expression is less than $\epsilon/2$.

Therefore, for all $k > \max(K_1, K_2)$,

$$\begin{aligned} &\left| \tilde{w}_{k-d}^{k,\gamma} - \sum_{i=1}^k (-1)^{i+1} e^{\alpha i(d-i/2+1/2)} \right| \\ &\leq \frac{k}{2} \cdot e^{\alpha(k/2)(d-k/4+1/2)} + \frac{k^2}{4} \cdot e^{\alpha(d-d/2+1/2)-(k/2+1)} \\ &\leq \epsilon/2 + \epsilon/2 = \epsilon. \end{aligned}$$

Thus, we have shown that $\tilde{w}_j^{k,\gamma}$ has a limit, and the limit is

$$\begin{aligned} \check{w}_d^\gamma &= \lim_{\substack{k \rightarrow \infty, j \rightarrow \infty, \\ k-j=d}} \tilde{w}_j^{k,\gamma} \\ &= \sum_{i=1}^{\infty} (-1)^{i+1} e^{\alpha i(d-i/2+1/2)}. \quad \square \end{aligned}$$

Now, we show that this form we just proved is the same as (12) to finish the proof of the property (a). Using the difference of squares formula,

$$\begin{aligned} \sum_{i=1}^{\infty} (-1)^{i+1} e^{\alpha i(d-i/2+1/2)} &= \sum_{i=1}^{\infty} (-1)^{i+1} e^{(\alpha/2)[(d+1/2)^2 - (i-(d+1/2))^2]} \\ &= e^{(\alpha/2)(d+1/2)^2} \sum_{i=1}^{\infty} (-1)^{i+1} e^{-(\alpha/2)(i-(d+1/2))^2}. \end{aligned}$$

However, we can cancel some terms in the following way. For $d \geq 0$,

$$\sum_{i=1}^{2d} (-1)^{i+1} e^{-(\alpha/2)(i-(d+1/2))^2} = \sum_{i=1}^d (-1)^{i+1} \left(e^{-(\alpha/2)(i-(d+1/2))^2} - e^{-(\alpha/2)((d+1/2)-i)^2} \right) = 0. \quad (21)$$

Similarly, for $d < 0$,

$$\sum_{i=0}^{2d+1} (-1)^{i+1} e^{-(\alpha/2)(i-(d+1/2))^2} = 0. \quad (22)$$

Therefore, using the cancellation of (21) and (22),

$$\begin{aligned} & e^{(\alpha/2)(d+1/2)^2} \sum_{i=1}^{\infty} (-1)^{i+1} e^{-(\alpha/2)(i-(d+1/2))^2} \\ &= e^{(\alpha/2)(d+1/2)^2} \sum_{i=2d+1}^{\infty} (-1)^{i+1} e^{-(\alpha/2)(i-(d+1/2))^2} \\ &= e^{(\alpha/2)(d+1/2)^2} \sum_{i=0}^{\infty} (-1)^{i+(2d+1)+1} e^{-(\alpha/2)(i+(2d+1)-(d+1/2))^2} \\ &= \sum_{i=0}^{\infty} (-1)^i e^{-\alpha i(d+i/2+1/2)}. \end{aligned}$$

To prove property (b), using the closed form from (12), note that

$$\begin{aligned} 1 - \check{w}_{-(d+1)}^\gamma &= 1 - \sum_{i=1}^{\infty} (-1)^{i+1} e^{\alpha i(-(d+1)-i/2+1/2)} \\ &= 1 + \sum_{i=1}^{\infty} (-1)^i e^{-\alpha i(d+i/2+1/2)} \\ &= \sum_{i=0}^{\infty} (-1)^i e^{-\alpha i(d+i/2+1/2)} \\ &= \check{w}_d^\gamma. \end{aligned}$$

Therefore, \check{w}_d^γ satisfies symmetry property $\check{w}_d^\gamma = 1 - \check{w}_{-(d+1)}^\gamma$.

To prove property (c), by basic asymptotic results, we write the bounds from (11) as

$$\begin{aligned} \lim_{\substack{k \rightarrow \infty, j \rightarrow \infty \\ k-j=d}} \frac{1 - e^{-\alpha k}}{1 - e^{-\alpha k} + e^{-\alpha(k-j)}} &= \frac{1}{1 + e^{-\alpha d}}, \text{ and} \\ \lim_{\substack{k \rightarrow \infty, j \rightarrow \infty \\ k-j=d}} \frac{1 - e^{-\alpha k}}{1 - e^{-\alpha k} + e^{-\alpha(k-j+1)}} &= \frac{1}{1 + e^{-\alpha(d+1)}}. \end{aligned}$$

Therefore, \check{w}_d^γ satisfies

$$\frac{1}{1 + e^{-\alpha d}} \leq \check{w}_d^\gamma \leq \frac{1}{1 + e^{-\alpha(d+1)}}. \quad (23)$$

Additionally, using the bounds from (23), we have

$$\check{w}_d^\gamma \leq \frac{1}{1 + e^{-\alpha(d+1)}} \leq \check{w}_{d+1}^\gamma, \quad (24)$$

demonstrating that \check{w}_d^γ is non-decreasing for $d \in \mathbb{Z}$. The inequality $\check{w}_d^\gamma \geq \frac{1}{1 + e^{-\alpha(d+1/2)}}$ for $d \geq 0$ follows directly from (30). Furthermore, we obtain $\check{w}_d^\gamma \leq \frac{1}{1 + e^{-\alpha(d+1/2)}}$ for $d < 0$ by using the relation $\check{w}_d^\gamma = 1 - \check{w}_{-(d+1)}^\gamma$.

To prove property (d), note that property (i) in the footnote follows immediately from (24). Next, we prove properties (ii) and (iii) in the footnote. To this end, using the two different series representations (12) and (18) of \check{w}_d^γ for integer d , we extend the definition of \check{w}_d^γ to all real d as follows. When $d < -1/2$, let $\check{w}_d^\gamma = \sum_{i=1}^{\infty} (-1)^{i+1} e^{\alpha i(d-i/2+1/2)}$ and when $d \geq -1/2$, let $\check{w}_d^\gamma = \sum_{i=0}^{\infty} (-1)^i e^{-\alpha i(d+i/2+1/2)}$. For $d > -1/2$, note that \check{w}_d^γ has second derivative

$$\frac{\partial^2}{\partial d^2} \check{w}_d^\gamma = \alpha^2 \sum_{i=0}^{\infty} (-1)^i i^2 e^{-\alpha i(d+i/2+1/2)} = \alpha^2 \sum_{i=0}^{\infty} (-1)^i z^{2i} i^2 q^{i^2}, \quad (25)$$

and $z, q \in (0, 1)$, where $q = e^{-\alpha/2}$ and $z = e^{-(\alpha/2)(d+1/2)}$. Now, consider the following identity from [18, Proposition 1.1]:

$$\sum_{i=0}^{\infty} (-1)^i z^{2i} q^{i^2} = \frac{1}{1+z} \sum_{i=0}^{\infty} z^i \prod_{j=0}^{i-1} \frac{1-zq^j}{1+zq^{j+1}}, \quad |z| < 1, |q| \leq 1. \quad (26)$$

Differentiating both sides of (26) with respect to q gives

$$\sum_{i=0}^{\infty} (-1)^i z^{2i} i^2 q^{i^2-1} = \frac{1}{1+z} \sum_{i=1}^{\infty} z^i \frac{\partial}{\partial q} \prod_{j=0}^{i-1} \frac{1-zq^j}{1+zq^{j+1}}. \quad (27)$$

By the product rule and quotient rule on (27),

$$\frac{\partial}{\partial q} \prod_{j=0}^{i-1} \frac{1-zq^j}{1+zq^{j+1}} = \sum_{l=0}^{i-1} \frac{q^{l-1} z (q^{l+1} z - l(q+1) - q)}{(1+zq^{l+1})^2} \prod_{0 \leq j \leq i-1, j \neq l} \frac{1-zq^j}{1+zq^{j+1}}. \quad (28)$$

Since $q^{l+1} z - l(q+1) - q \leq 0$ for all $l \geq 0$ and $(1-zq^j)/(1+zq^{j+1}) \geq 0$ for all $j \geq 0$ when $z, q \in [0, 1)$, it follows that (28) is non-positive, implying the same for (27). Returning to (25), we deduce that \check{w}_d^γ is concave for all $d > -1/2$. An analogous argument shows that \check{w}_d^γ is convex for $d < -1/2$. This proves properties (ii) and (iii) in the footnote when $d \neq -1, 0$. For the $d = -1, 0$ cases, we have from the just established convexity/concavity and continuity that

$$\begin{aligned} \frac{1}{3} \check{w}_{-2}^\gamma + \frac{2}{3} \lim_{d \uparrow -1/2} \check{w}_d^\gamma &\geq \check{w}_{-1}^\gamma, \\ \frac{2}{3} \check{w}_{-1/2}^\gamma + \frac{1}{3} \check{w}_1^\gamma &\leq \check{w}_0^\gamma, \end{aligned} \quad (29)$$

where $\lim_{d \uparrow -1/2} \check{w}_d^\gamma = 1 - \check{w}_{-1/2}^\gamma$. We will show that these equations (29) together imply properties (ii) and (iii) in the footnote when $d = -1, 0$. Expanding the power series (26), one obtains

$$\check{w}_d^\gamma = \frac{1}{1+z} \sum_{i=0}^{\infty} z^i \prod_{j=0}^{i-1} \frac{1-zq^j}{1+zq^{j+1}} \geq \frac{1}{1+z} \sum_{i=0}^{\infty} z^i \prod_{j=0}^{i-1} \frac{1-z}{1+z} = \frac{1}{1+z^2} = \frac{1}{1+e^{-\alpha(d+1/2)}}. \quad (30)$$

Thus, we have $\check{w}_{-1/2}^\gamma \geq 1/2$ and hence $\check{w}_{-1/2}^\gamma \geq \lim_{d \uparrow -1/2} \check{w}_d^\gamma$. Thus, from (29), we obtain

$$3\check{w}_{-1}^\gamma + \check{w}_1^\gamma \leq 3\check{w}_0^\gamma + \check{w}_{-2}^\gamma. \quad (31)$$

Finally, the identity $\check{w}_d^\gamma = 1 - \check{w}_{-(d+1)}^\gamma$ for $d \in \mathbb{Z}$ from part (c) of Theorem 4.2 applied to (31) yields properties (ii) and (iii) in the footnote when $d = -1, 0$. \square

Proof of Theorem 4.3. We leave the proof to the end of Section A.3. \square

A.3 Proof for Error Improvement

Proof of Theorem 3.2. From the decompositions (5) and (4), we have the following identity

$$\|\mathbf{y} - \hat{\mathbf{f}}_{k,p}\|^2 - \|\mathbf{y} - \hat{\mathbf{f}}_{k,m_p,p}\|^2 = \sum_{j=k+1}^p \hat{\beta}_{j,p}^2 \left(1 - \left(-w_j^{k,m_p,p}\right)^2\right) - \sum_{j=1}^k \hat{\beta}_{j,p}^2 \left(1 - w_j^{k,m_p,p}\right)^2. \quad (32)$$

Let $m_p = \lfloor \gamma p \rfloor$, where $0 < \gamma < 1$. Then, using (32), we have

$$\begin{aligned} & \mathbb{E} \left[\|\mathbf{y} - \hat{\mathbf{f}}_{k,p}\|^2 - \min_m \|\mathbf{y} - \hat{\mathbf{f}}_{k,m,p}\|^2 \right] \\ & \geq \sum_{j=k+1}^{2k} \mathbb{E}[\hat{\beta}_{j,p}^2] \left(1 - \left(-w_j^{k,m_p,p}\right)^2\right) - \sum_{j=1}^k \mathbb{E}[\hat{\beta}_{j,p}^2] \left(1 - w_j^{k,m_p,p}\right)^2. \end{aligned} \quad (33)$$

To simplify further, we use Chebyshev's sum inequality [31], noting that $\mathbb{E}[\hat{\beta}_{j,p}^2]$ is non-increasing in j by definition and $w_j^{k,m_p,p}$ is non-increasing in j by Theorem 4.1. Thus, the second term in (33) is upper bounded by

$$\sum_{j=1}^k \mathbb{E}[\hat{\beta}_{j,p}^2] \left(1 - w_j^{k,m_p,p}\right)^2 \leq \left(\frac{1}{k} \sum_{j=1}^k \mathbb{E}[\hat{\beta}_{j,p}^2]\right) \left(\sum_{j=1}^k \left(1 - w_j^{k,m_p,p}\right)^2\right),$$

and the first term in (33) is lower bounded by

$$\begin{aligned} & \sum_{j=k+1}^{2k} \mathbb{E}[\hat{\beta}_{j,p}^2] \left(1 - \left(-w_j^{k,m_p,p}\right)^2\right) \\ & \geq \left(\frac{1}{k} \sum_{j=k+1}^{2k} \mathbb{E}[\hat{\beta}_{j,p}^2]\right) \left(\sum_{j=k+1}^{2k} \left(1 - \left(-w_j^{k,m_p,p}\right)^2\right)\right). \end{aligned}$$

We claim that for a fixed k and a sequence $\{\gamma_p\}$ that depends on both p and k , with $\gamma_p \geq C > 0$ where C is some constant depending on k , if we set $m_p = \lfloor \gamma_p p \rfloor$, then there exists a constant $C(k, \epsilon)$ such that when $p(1 - \gamma_p)^3 \geq C(k, \epsilon)$,

$$\sum_{j=k+1}^{2k} \left(1 - \left(-w_j^{k,m_p,p}\right)^2\right) \geq (1 - \epsilon) \sum_{j=k+1}^{2k} \left(1 - \left(-\tilde{w}_j^{k,\gamma_p}\right)^2\right), \quad (34)$$

and

$$\sum_{j=1}^k \left(1 - w_j^{k,m_p,p}\right)^2 \leq (1 + \epsilon) \sum_{j=1}^k \left(1 - \tilde{w}_j^{k,\gamma_p}\right)^2. \quad (35)$$

For simplicity of notation, throughout the proof of this theorem, we use the notation " $A \lesssim B$ " to mean that there exists a constant C depending on k such that $A \leq CB$. To prove the claim, we first show that when $p(1 - \gamma_p)^2$ is sufficiently large,

$$\left| \frac{\sum_{j=k+1}^{2k} \left(1 - \left(-w_j^{k,m_p,p}\right)^2\right) - \sum_{j=k+1}^{2k} \left(1 - \left(-\tilde{w}_j^{k,\gamma_p}\right)^2\right)}{\sum_{j=k+1}^{2k} \left(1 - \left(-\tilde{w}_j^{k,\gamma_p}\right)^2\right)} \right| \lesssim \frac{1}{p(1 - \gamma_p)^2}. \quad (36)$$

If (36) holds, then it is clear that the claim for (34) holds.

To prove (36), we revisit the proof of Lemma A.1. Note that

$$\frac{\binom{p-j}{m_p-1}}{\binom{p}{m_p}} = \frac{m_p}{p-j-m_p+1} \prod_{i=1}^j \frac{i+p-m_p}{i+p} = \frac{1+p-m_p}{p-j-m_p+1} \frac{m_p}{1+p} \prod_{i=2}^j \frac{i+p-m_p}{i+p}.$$

For a fixed $2 \leq j \leq 2k$, we have that for any $2 \leq i \leq j$, $\left| \frac{i+p-m_p}{i+p} - (1-\gamma_p) \right| \lesssim \frac{1}{p+i}$. Additionally, $\left| \frac{m_p}{1+p} - \gamma_p \right| \lesssim \frac{1}{p+1}$. Thus, we know when p is sufficiently large, $\left| \frac{m_p}{1+p} \prod_{i=2}^j \frac{i+p-m_p}{i+p} - \gamma_p (1-\gamma_p)^{j-1} \right| \lesssim \frac{1}{p+1}$. Next, we observe that when $p(1-\gamma_p)$ is sufficiently large,

$$\frac{1+p-m_p}{p-j-m_p+1} - 1 = \frac{j}{p-j-m_p+1} \lesssim \frac{1}{p(1-\gamma_p)}.$$

Therefore, when $p(1-\gamma_p)$ is sufficiently large, we have

$$\left| \frac{\binom{p-j}{m_p-1}}{\binom{p}{m_p}} - \gamma_p (1-\gamma_p)^{j-1} \right| \lesssim \frac{1}{p(1-\gamma_p)}.$$

Additionally, using a similar analysis, we know that when $p(1-\gamma_p)$ is sufficiently large,

$$\left| \frac{\binom{p-j}{m_p}}{\binom{p}{m_p}} - (1-\gamma_p)^j \right| = \left| \prod_{i=0}^{j-1} \frac{p-m_p-i}{p-i} - (1-\gamma_p)^j \right| \lesssim \frac{1}{p},$$

and

$$\left| \frac{\binom{p-j+1}{m_p}}{\binom{p}{m_p}} - (1-\gamma_p)^{j-1} \right| \lesssim \frac{1}{p(1-\gamma_p)}.$$

According to the recurrence (9) and the fact that $w_j^{0,m_p,p} = 0$ for all j and all p , we conclude that for any $1 \leq j \leq 2k$, the quantity $w_j^{k,m_p,p}$ can be determined through a finite number of recursive steps (depending on k). In other words, the approximation error $|w_j^{k,m_p,p} - \tilde{w}_j^{k,\gamma_p}|$ accumulates only over a finite number of recursive steps (depending on k). Therefore, for any $1 \leq j \leq 2k$, when $p(1-\gamma_p)$ is sufficiently large, we have the error bound $|w_j^{k,m_p,p} - \tilde{w}_j^{k,\gamma_p}| \lesssim \frac{1}{p(1-\gamma_p)}$. Thus, it holds that

$$\left| \sum_{j=k+1}^{2k} \left(1 - (-w_j^{k,m_p,p})^2 \right) - \sum_{j=k+1}^{2k} \left(1 - (-\tilde{w}_j^{k,\gamma_p})^2 \right) \right| \lesssim \frac{1}{p(1-\gamma_p)}. \quad (37)$$

Next, we show that when $\gamma_p \gtrsim 1$, it holds that

$$\sum_{j=k+1}^{2k} \left(1 - (-\tilde{w}_j^{k,\gamma_p})^2 \right) \gtrsim 1 - \gamma_p. \quad (38)$$

To lower bound $\sum_{j=k+1}^{2k} \left(1 - \left(-\tilde{w}_j^{k,\gamma_p}\right)^2\right)$ from (38), note that

$$1 - \left(1 - \tilde{w}_j^{k,\gamma_p}\right)^2 = \tilde{w}_j^{k,\gamma_p} \left(2 - \tilde{w}_j^{k,\gamma_p}\right),$$

so we wish to have simple upper and lower bounds on \tilde{w}_j^{k,γ_p} for $j \geq k+1$ to lower bound each $1 - \left(1 - \tilde{w}_j^{k,\gamma_p}\right)^2$. Recall that $1 - \gamma_p = e^{-\alpha_p}$. Since $j \geq k+1$, we have the following lower bound \tilde{w}_j^{k,γ_p} from (11):

$$\tilde{w}_j^{k,\gamma_p} \geq \frac{1 - e^{-\alpha_p k}}{1 - e^{-\alpha_p k} + e^{-\alpha_p(k-j)}} \geq e^{-\alpha_p(j-k)} \frac{1 - e^{-\alpha_p k}}{1 + e^{-\alpha_p}}, \quad j \geq k+1. \quad (39)$$

Now, from (11), observe that for all $j \geq k+1$,

$$\tilde{w}_j^{k,\gamma_p} \leq \frac{1 - e^{-\alpha_p k}}{1 - e^{-\alpha_p k} + e^{-\alpha_p(k-j+1)}} \leq \frac{1 - e^{-\alpha_p k}}{1 - e^{-\alpha_p k} + 1} \leq 1/2. \quad (40)$$

From (39) and (40), we obtain

$$1 - \left(1 - \tilde{w}_j^{k,\gamma_p}\right)^2 = \tilde{w}_j^{k,\gamma_p} \left(2 - \tilde{w}_j^{k,\gamma_p}\right) \geq \frac{3}{2} e^{-\alpha_p(j-k)} \frac{1 - e^{-\alpha_p k}}{1 + e^{-\alpha_p}}, \quad j \geq k+1. \quad (41)$$

Substituting in (41), we thus have

$$\sum_{j=k+1}^{2k} \left(1 - \left(-\tilde{w}_j^{k,\gamma_p}\right)^2\right) \geq \frac{3}{2} e^{-\alpha_p} \frac{1 - e^{-\alpha_p k}}{1 - e^{-\alpha_p}} \frac{1 - e^{-\alpha_p k}}{1 + e^{-\alpha_p}} = \frac{3}{2} \frac{e^{-\alpha_p} (1 - e^{-\alpha_p k})^2}{1 - e^{-2\alpha_p}}. \quad (42)$$

Noting that $\gamma_p \gtrsim$ implies $\alpha_p \gtrsim 1$, we obtain

$$\sum_{j=k+1}^{2k} \left(1 - \left(-\tilde{w}_j^{k,\gamma_p}\right)^2\right) \geq \frac{3}{2} e^{-\alpha_p} (1 - e^{-\alpha_p k})^2 \gtrsim e^{-\alpha_p} = 1 - \gamma_p,$$

which establishes (38). Combining (37) and (38) proves (36), which in turn confirms (34).

To prove (35), we show that when $\gamma_p \gtrsim 1$,

$$\sum_{j=1}^k \left(1 - \tilde{w}_j^{k,\gamma_p}\right)^2 \gtrsim (1 - \gamma_p)^2. \quad (43)$$

When $p(1 - \gamma_p)^3$ is sufficiently large, if (43) holds, then using the fact that $\left|w_j^{k,m_p,p} - \tilde{w}_j^{k,\gamma_p}\right| \lesssim \frac{1}{p(1 - \gamma_p)}$, we know

$$\frac{\left|\sum_{j=1}^k \left(1 - w_j^{k,m_p,p}\right)^2 - \sum_{j=1}^k \left(1 - \tilde{w}_j^{k,\gamma_p}\right)^2\right|}{\sum_{j=1}^k \left(1 - \tilde{w}_j^{k,\gamma_p}\right)^2} \lesssim \frac{1}{p(1 - \gamma_p)^3},$$

which implies (35).

Note that from (11), we have

$$\tilde{w}_j^{k,\gamma_p} \leq \frac{1 - e^{-\alpha_p k}}{1 - e^{-\alpha_p k} + e^{-\alpha_p(k-j+1)}} \leq \frac{1}{1 + e^{-\alpha_p(k-j+1)}}.$$

Thus,

$$\sum_{j=1}^k \left(1 - \tilde{w}_j^{k,\gamma_p}\right)^2 \geq \sum_{j=1}^k \frac{e^{-2\alpha_p(k-j+1)}}{\left(1 + e^{-\alpha_p(k-j+1)}\right)^2} \geq \frac{1}{4} \sum_{j=1}^k e^{-2\alpha_p(k-j+1)} = \frac{e^{-2\alpha_p}(1 - e^{-2\alpha_p k})}{4(1 - e^{-2\alpha_p})}.$$

Noting that $\gamma_p \gtrsim$ implies $\alpha_p \gtrsim 1$, we obtain (43).

Therefore, the claim is proven for (34) and (35). To upper bound the sum $\sum_{j=1}^k \left(1 - \tilde{w}_j^{k,\gamma_p}\right)^2$ from (35), we use the following rearranged version of recurrence (17):

$$1 - \tilde{w}_j^{k,\gamma_p} = e^{-\alpha_p k} (1 - \tilde{w}_{j-1}^{k,\gamma_p}) + e^{-\alpha_p(k-j+1)} \tilde{w}_{j-1}^{k,\gamma_p}. \quad (44)$$

Upon squaring both sides of (44), we obtain

$$\begin{aligned} \left(1 - \tilde{w}_j^{k,\gamma_p}\right)^2 &= e^{-2\alpha_p k} \left(1 - \tilde{w}_{j-1}^{k,\gamma_p}\right)^2 + \\ &\quad 2e^{-\alpha_p(2k-j+1)} \tilde{w}_{j-1}^{k,\gamma_p} (1 - \tilde{w}_{j-1}^{k,\gamma_p}) + e^{-2\alpha_p(k-j+1)} \left(\tilde{w}_{j-1}^{k,\gamma_p}\right)^2. \end{aligned} \quad (45)$$

Summing (45) over $1 \leq j \leq k$, using the Cauchy-Schwarz inequality, and the fact from Theorem 4.1 that $\tilde{w}_{j-1}^{k,\gamma_p} \geq \tilde{w}_j^{k,\gamma_p}$, we obtain

$$\begin{aligned} \sum_{j=1}^k \left(1 - \tilde{w}_j^{k,\gamma_p}\right)^2 &\leq e^{-2\alpha_p k} \sum_{j=1}^k \left(1 - \tilde{w}_{j-1}^{k,\gamma_p}\right)^2 \\ &\quad + 2e^{-\alpha_p k} \sqrt{\sum_{j=1}^k \left(1 - \tilde{w}_{j-1}^{k,\gamma_p}\right)^2 \sum_{j=1}^k e^{-2\alpha_p(k-j+1)} \left(\tilde{w}_{j-1}^{k,\gamma_p}\right)^2} \\ &\quad + \sum_{j=1}^k e^{-2\alpha_p(k-j+1)} \left(\tilde{w}_{j-1}^{k,\gamma_p}\right)^2 \\ &\leq e^{-2\alpha_p k} \sum_{j=1}^k \left(1 - \tilde{w}_j^{k,\gamma_p}\right)^2 \\ &\quad + 2e^{-\alpha_p k} \sqrt{\sum_{j=1}^k \left(1 - \tilde{w}_j^{k,\gamma_p}\right)^2 \sum_{j=1}^k e^{-2\alpha_p(k-j+1)} \left(\tilde{w}_{j-1}^{k,\gamma_p}\right)^2} \\ &\quad + \sum_{j=1}^k e^{-2\alpha_p(k-j+1)} \left(\tilde{w}_{j-1}^{k,\gamma_p}\right)^2. \end{aligned} \quad (46)$$

Solving the quadratic inequality (46) yields

$$\sum_{j=1}^k \left(1 - \tilde{w}_j^{k,\gamma_p}\right)^2 \leq \frac{\sum_{j=1}^k e^{-2\alpha_p(k-j+1)} \left(\tilde{w}_{j-1}^{k,\gamma_p}\right)^2}{(1 - e^{-\alpha_p k})^2}. \quad (47)$$

Now, from the upper bound (11), we have $(\tilde{w}_{j-1}^{k,\gamma_p})^2 \leq (1 - e^{-\alpha_p k})^2$ for all $j \geq 1$. Substituting this into (47), we obtain the bound

$$\sum_{j=1}^k (1 - \tilde{w}_j^{k,\gamma_p})^2 \leq \sum_{j=1}^k e^{-2\alpha_p(k-j+1)} = \frac{e^{-2\alpha_p}(1 - e^{-2\alpha_p k})}{1 - e^{-2\alpha_p}}. \quad (48)$$

To simplify notation, set

$$A = \frac{1}{k} \sum_{j=1}^k \mathbb{E}[\hat{\beta}_{j,p}^2], \quad B = \frac{1}{k} \sum_{j=k+1}^{2k} \mathbb{E}[\hat{\beta}_{j,p}^2], \quad (49)$$

and note that $A \geq B$ by applying Definition 3.1. Using (49) and by the previous inequalities in (48) and (42), the training error gap (33) is at least

$$\begin{aligned} & \frac{3}{2}(1 - \epsilon)B \frac{e^{-\alpha_p}(1 - e^{-\alpha_p k})^2}{1 - e^{-2\alpha_p}} - A(1 + \epsilon) \frac{e^{-2\alpha_p}(1 - e^{-2\alpha_p k})}{1 - e^{-2\alpha_p}} \\ &= \left(\frac{1 - e^{-\alpha_p k}}{1 - e^{-\alpha_p}} \right) \left[\frac{3}{2}(1 - \epsilon)B \frac{e^{-\alpha_p}(1 - e^{-\alpha_p k})}{1 + e^{-\alpha_p}} - (1 + \epsilon)A \frac{e^{-2\alpha_p}(1 + e^{-\alpha_p k})}{1 + e^{-\alpha_p}} \right] \\ &\geq \frac{3}{2}(1 - \epsilon)B e^{-\alpha_p} \frac{1 - e^{-\alpha_p}}{1 + e^{-\alpha_p}} - (1 + \epsilon)A e^{-2\alpha_p} \\ &\geq \frac{3}{2}(1 - \epsilon)B e^{-\alpha_p} \frac{1 - e^{-\alpha_0}}{1 + e^{-\alpha_0}} - (1 + \epsilon)A e^{-2\alpha_p}, \end{aligned} \quad (50)$$

for any $\alpha_0 \leq \alpha_p$. Take α_p^* such that

$$\alpha_p^* = \log \left(\frac{4}{3} \cdot \frac{1 + e^{-\alpha_0^*}}{1 - e^{-\alpha_0^*}} \cdot \frac{A}{B} \right),$$

where the corresponding γ_p^* is given by $\gamma_p^* = 1 - e^{-\alpha_p^*}$, and $\alpha_0^* = (7 + \sqrt{97})/6$. It is straightforward to verify that

$$\alpha_p^* = \log \left(\frac{4}{3} \cdot \frac{1 + e^{-\alpha_0^*}}{1 - e^{-\alpha_0^*}} \cdot \frac{A}{B} \right) \geq \log \left(\frac{4}{3} \cdot \frac{1 + e^{-\alpha_0^*}}{1 - e^{-\alpha_0^*}} \right) = \alpha_0^*.$$

Thus, substituting α_p^* and α_0^* into (50) and taking $\epsilon = 0.05$ gives us the lower bound on expected training error gap (33) as

$$\begin{aligned} & \left(\frac{3}{4} \right) \left(\frac{3}{4} - \frac{9}{4}\epsilon \right) \left(\frac{1 - e^{-\alpha_0^*}}{1 + e^{-\alpha_0^*}} \right)^2 \frac{\left(\frac{1}{k} \sum_{j=k+1}^{2k} \mathbb{E}[\hat{\beta}_{j,p}^2] \right)^2}{\frac{1}{k} \sum_{j=1}^k \mathbb{E}[\hat{\beta}_{j,p}^2]} \\ &\geq \frac{1}{4} \frac{\left(\frac{1}{k} \sum_{j=k+1}^{2k} \mathbb{E}[\hat{\beta}_{j,p}^2] \right)^2}{\frac{1}{k} \sum_{j=1}^k \mathbb{E}[\hat{\beta}_{j,p}^2]}. \end{aligned}$$

Therefore, for any fixed $k \geq 1$, when $p(1 - \gamma_p^*)^3 \gtrsim 1$, we have

$$\mathbb{E} \left[\|\mathbf{y} - \hat{\mathbf{f}}_{k,p}\|^2 - \min_m \|\mathbf{y} - \hat{\mathbf{f}}_{k,m,p}\|^2 \right] \geq \frac{1}{4} \frac{\left(\frac{1}{k} \sum_{j=k+1}^{2k} \mathbb{E}[\hat{\beta}_{j,p}^2] \right)^2}{\frac{1}{k} \sum_{j=1}^k \mathbb{E}[\hat{\beta}_{j,p}^2]}. \quad \square$$

A.3.1 Proofs for Degrees of Freedom Results

Proof of Theorem 3.1. Note that for $k = 1, 2, \dots, p$, we have

$$\hat{f}_{k,m,p} = \sum_{j=1}^p w_j^{k,m,p} \hat{\beta}_{j,p} x_{j,p}, \quad \hat{f}_{k,p} = \sum_{j=1}^k \hat{\beta}_{j,p} x_{j,p},$$

which implies

$$\hat{f}_{k,m,p} = \sum_{j=1}^p w_j^{k,m,p} (\hat{f}_{j,p} - \hat{f}_{j-1,p}).$$

Since degrees of freedom is a linear operator over estimators, we have

$$\text{df}(\hat{f}_{k,m,p}) = \sum_{j=1}^p w_j^{k,m,p} \Delta(j), \quad (51)$$

where $\Delta(j) := \text{df}(\hat{f}_{j,p}) - \text{df}(\hat{f}_{j-1,p})$, for $j = 1, 2, \dots, p$, forms a non-increasing sequence by the concavity assumption. We claim that whenever $m' > m$, the sequence $\{w_j^{k,m',p}\}_{j=1}^p$ majorizes the sequence $\{w_j^{k,m,p}\}_{j=1}^p$. This means that for each $l \geq 1$,

$$\sum_{j=1}^l w_j^{k,m',p} \geq \sum_{j=1}^l w_j^{k,m,p}, \quad (52)$$

with equality when $l = p$.

Assuming the majorization in (52) holds, the theorem follows directly from Theorem A.3 in [39] by using the facts that both $w_j^{k,m',p}$ and $\Delta(j)$ are non-increasing in j .

We return to proving the claim. Let $S_{k,m,p}$ denote the indices of the features selected by one inner loop of RGS with parameters k , m , and p . We may write

$$\begin{aligned} \sum_{j=1}^l w_j^{k,m,p} &= \sum_{j=1}^l \mathbb{P}(j \in S_{k,m,p}) \\ &= \mathbb{E} \left[\sum_{j=1}^l \mathbb{1}(j \in S_{k,m,p}) \right] \\ &= \mathbb{E}[Z_{k,m,p}(l)], \end{aligned}$$

where $Z_{k,m,p}(l) := |S_{k,m,p} \cap [l]|$. Evidently, (52) will be established if we can produce a coupling between $S_{k,m,p}$ and $S_{k,m',p}$ such that $Z_{k,m',p}(l) \geq Z_{k,m,p}(l)$ for $l = 1, 2, \dots, p$.

We construct such a coupling by running two instances of RGS concurrently, one with parameter choice m and the other with parameter choice m' . At iteration $k + 1$ of the algorithm, we first draw a subset B_m of size m from $[p - k]$ uniformly at random. We then draw a further subset of $m' - m$ elements from $[p - k] \setminus B_m$ uniformly at random and take their union with B_m to form $B_{m'}$. We then construct the candidate subset $\mathcal{V}_{k+1,m,p}$

by ordering $[p] \setminus S_{k,m,p}$ from smallest to largest and picking the elements at positions in B_m . To construct the candidate subset $\mathcal{V}_{k+1,m',p}$, we do the same, but with $[p] \setminus S_{k,m',p}$ and $B_{m'}$ instead of $[p] \setminus S_{k,m,p}$ and B_m respectively.

We now show the desired property inductively in k , with the base case $k = 0$ trivial. Assume the inductive hypothesis. Let $b := \min B_m$. Then one can show that the index selected at iteration $k + 1$ (with parameter m) is equal to $l_* := \min\{l: b \leq l - Z_{k,m,p}(l)\}$. We therefore have

$$Z_{k+1,m,p}(l) = \begin{cases} Z_{k,m,p}(l) & \text{if } l < l_* \\ Z_{k,m,p}(l) + 1 & \text{if } l \geq l_*. \end{cases}$$

Similarly, denoting $b' := \min B_{m'}$ and letting $l'_* := \min\{l: b' \leq l - Z_{k,m',p}(l)\}$, we get

$$Z_{k+1,m',p}(l) = \begin{cases} Z_{k,m',p}(l) & \text{if } l < l'_* \\ Z_{k,m',p}(l) + 1 & \text{if } l \geq l'_*. \end{cases}$$

To compare $Z_{k+1,m',p}$ and $Z_{k,m,p}$, we further set $\tilde{l} := \min\{l: b \leq l - Z_{k,m',p}(l)\}$ and construct the function \tilde{Z} via

$$\tilde{Z}(l) = \begin{cases} Z_{k,m',p}(l) & \text{if } l < \tilde{l} \\ Z_{k,m',p}(l) + 1 & \text{if } l \geq \tilde{l}. \end{cases}$$

Since $b' \leq b$, we have $\tilde{l} \geq l'_*$, so that $\tilde{Z} \leq Z_{k+1,m',p}$. Next, notice that

$$\tilde{Z}(l) - Z_{k+1,m,p}(l) = \begin{cases} Z_{k,m',p}(l) - Z_{k,m,p}(l) & \text{if } l < l_* \\ Z_{k,m',p}(l) - Z_{k,m,p}(l) - 1 & \text{if } l_* \leq l < \tilde{l} \\ Z_{k,m',p}(l) - Z_{k,m,p}(l) & \text{if } l \geq \tilde{l}. \end{cases}$$

By the induction hypothesis, we have $Z_{k,m',p}(l) - Z_{k,m,p}(l) \geq 0$. Meanwhile, on $l_* \leq l < \tilde{l}$, write

$$Z_{k,m',p}(l) - Z_{k,m,p}(l) = (Z_{k,m',p}(l) - l) - (Z_{k,m,p}(l) - l). \quad (53)$$

Because these functions take integral values, the only way $Z_{k,m',p}(l) - Z_{k,m,p}(l) - 1$ can be negative is if the right hand side of (53) is equal to 0. However, by the way in which l_* is defined, we would have

$$l - Z_{k,m',p}(l) = l - Z_{k,m,p}(l) \geq b,$$

which contradicts the definition of \tilde{l} . This implies that $Z_{k+1,m,p} \leq \tilde{Z}$, which when combined with the earlier comparison, gives $Z_{k+1,m,p} \leq Z_{k+1,m',p}$ as desired. \square

Utilizing the majorization in (52), we now turn to prove Theorem 4.3.

Proof of Theorem 4.3. According to the decomposition (5), it suffices to prove

$$\sum_{j=1}^p \hat{\beta}_{j,p}^2 (w_j^{k,m,p})^2 \leq \sum_{j=1}^p \hat{\beta}_{j,p}^2 (w_j^{k,m',p})^2. \quad (54)$$

Applying Proposition A.3.a from [39], where in their notation we take $p_j = \hat{\beta}_{j,p}^2$ and $g(x) = x^2$, noting that g is an increasing convex function on the positive real numbers, it follows that (54) holds if for any $l \geq 1$,

$$\sum_{j=1}^l \hat{\beta}_{j,p}^2 w_j^{k,m,p} \leq \sum_{j=1}^l \hat{\beta}_{j,p}^2 w_j^{k,m',p}. \quad (55)$$

Applying Theorem A.3 from [39] and using the fact that $\hat{\beta}_{j,p}^2$ is non-increasing in j , we conclude that (55) holds for any $l \geq 1$. \square

For the remaining proofs in this section, we depart from the notation used in the rest of this paper, and let $\mathbf{x}_{1,p}, \mathbf{x}_{2,p}, \dots, \mathbf{x}_{p,p}$ denote a *fixed* ordering of the features. Correspondingly, their regression coefficients $\hat{\beta}_{1,p}, \hat{\beta}_{2,p}, \dots, \hat{\beta}_{p,p}$ will no longer be assumed to be in sorted order.

Proof of Proposition 6.1. Consider any pair of distinct feature indices, $i \neq j$. Then

$$\hat{\beta}_{i,p} - \hat{\beta}_{j,p} = (\beta_{i,p} - \beta_{j,p}) + \langle \mathbf{x}_{i,p} - \mathbf{x}_{j,p}, \boldsymbol{\varepsilon} \rangle.$$

The second term has the distribution $\mathcal{N}(0, 2\sigma^2/n)$. In particular, if $i \leq k$ and $j > k$, we have

$$\mathbb{P}(\hat{\beta}_i - \hat{\beta}_j < 0) \leq (4\pi\sigma^2/n)^{-1/2} \exp(-n/4\sigma^2).$$

Similarly, we have

$$\mathbb{P}(\hat{\beta}_i + \hat{\beta}_j < 0) \leq (4\pi\sigma^2/n)^{-1/2} \exp(-n/4\sigma^2).$$

Putting these together gives

$$\begin{aligned} \mathbb{P}(|\hat{\beta}_{j,p}| > |\hat{\beta}_{i,p}|) &\leq \mathbb{P}(|\hat{\beta}_{j,p}| > \hat{\beta}_{i,p}) \\ &\leq \mathbb{P}(\hat{\beta}_{j,p} > \hat{\beta}_{i,p}) + \mathbb{P}(-\hat{\beta}_{j,p} < \hat{\beta}_{i,p}) \\ &\leq (\pi\sigma^2/n)^{-1/2} \exp(-n/4\sigma^2). \end{aligned}$$

Let \mathcal{A} be the event on which $\text{rank}(|\hat{\beta}_{j,p}| \leq k, \text{ for } j = 1, \dots, k)$. We have

$$\begin{aligned} \mathbb{P}(\mathcal{A}) &= \mathbb{P}(|\hat{\beta}_{i,p}| > |\hat{\beta}_{j,p}|, 1 \leq i \leq k < j \leq p) \\ &\geq 1 - k(p-k)(\pi\sigma^2/n)^{-1/2} \exp(-n/4\sigma^2). \end{aligned}$$

Next, let $\widetilde{\mathbf{H}}_k = n^{-1} \sum_{i=1}^k \mathbf{x}_{i,k} \mathbf{x}_{i,k}^\top$. This is the projection matrix onto the column span of the first k features. Let \mathbf{H}_k be the smoothing matrix corresponding to k steps of FS, noting that it depends on $\boldsymbol{\varepsilon} = (\varepsilon_1, \varepsilon_2, \dots, \varepsilon_n)$. Observe that on the event \mathcal{A} , we have $\widetilde{\mathbf{H}}_k = \mathbf{H}_k$. We can then write

$$\begin{aligned} \text{df}(\hat{f}_{k,p}) &= \frac{1}{\sigma^2} \mathbb{E}[\boldsymbol{\varepsilon}^\top \mathbf{H}_k \mathbf{y}] \\ &= \frac{1}{\sigma^2} \mathbb{E}[\boldsymbol{\varepsilon}^\top \mathbf{H}_k \mathbf{y} \cdot \mathbb{1}(\mathcal{A})] + \frac{1}{\sigma^2} \mathbb{E}[\boldsymbol{\varepsilon}^\top \mathbf{H}_k \mathbf{y} \cdot \mathbb{1}(\mathcal{A}^c)] \\ &= \frac{1}{\sigma^2} \mathbb{E}[\boldsymbol{\varepsilon}^\top \widetilde{\mathbf{H}}_k \mathbf{y}] - \frac{1}{\sigma^2} \mathbb{E}[\boldsymbol{\varepsilon}^\top \widetilde{\mathbf{H}}_k \mathbf{y} \cdot \mathbb{1}(\mathcal{A}^c)] + \frac{1}{\sigma^2} \mathbb{E}[\boldsymbol{\varepsilon}^\top \mathbf{H}_k \mathbf{y} \cdot \mathbb{1}(\mathcal{A}^c)]. \end{aligned}$$

The first term satisfies

$$\frac{1}{\sigma^2} \mathbb{E} \left[\boldsymbol{\varepsilon}^\top \widetilde{\mathbf{H}}_k \mathbf{y} \right] = \frac{1}{\sigma^2} \mathbb{E} \left[\boldsymbol{\varepsilon}^\top \widetilde{\mathbf{H}}_k \boldsymbol{\varepsilon} \right] = k.$$

To bound the third term, notice that since \mathbf{H}_k is a projection matrix, we can bound

$$\begin{aligned} \boldsymbol{\varepsilon}^\top \mathbf{H}_k \mathbf{y} &= \boldsymbol{\varepsilon}^\top \mathbf{H}_k \boldsymbol{\varepsilon} + \boldsymbol{\varepsilon}^\top \mathbf{H}_k \mathbf{f} \\ &\leq \|\boldsymbol{\varepsilon}\|_2^2 + \sqrt{kn} \|\boldsymbol{\varepsilon}\|_2. \end{aligned}$$

In particular, we get

$$\mathbb{E} \left[(\boldsymbol{\varepsilon}^\top \mathbf{H}_k \mathbf{y})^2 \right]^{1/2} \leq C(\sqrt{k} + \sigma) \sigma n,$$

where C is a universal constant. Applying Cauchy-Schwarz thus gives us

$$\begin{aligned} \frac{1}{\sigma^2} \mathbb{E} \left[\boldsymbol{\varepsilon}^\top \mathbf{H}_k \mathbf{y} \cdot \mathbb{1}(\mathcal{A}^c) \right] &\leq \frac{1}{\sigma^2} \mathbb{E} \left[(\boldsymbol{\varepsilon}^\top \mathbf{H}_k \mathbf{y})^2 \right]^{1/2} \mathbb{P}(\mathcal{A})^{1/2} \\ &\leq C(\sqrt{k}/\sigma + 1) nk(p-k)(\pi\sigma^2/n)^{-1/4} \exp(-n/8\sigma^2). \end{aligned}$$

By a similar calculation, the second term is bounded by the same value. Hence,

$$\text{df}(\hat{f}_{k,p}) = k + O(e^{-cn}).$$

Meanwhile, let τ denote the index of the feature selected on the $(k+1)$ -th step of FS. We then have $\hat{f}_{k+1,p} - \hat{f}_{k,p} = \hat{\beta}_{\tau,p} x_{\tau,p}$, which gives

$$\text{df}(\hat{f}_{k+1,p}) - \text{df}(\hat{f}_{k,p}) = \text{df}(\hat{\beta}_\tau \psi_\tau).$$

On the event \mathcal{A} , it is easy to see that

$$\tau = \arg \max_{k+1 \leq j \leq p} \hat{\beta}_{j,p}^2.$$

As such, we compute

$$\begin{aligned} \text{df}(\hat{\beta}_\tau \psi_\tau) &= \frac{1}{\sigma^2} \mathbb{E} \left[(\mathbf{y} - \mathbb{E} \mathbf{y})^\top \hat{\beta}_{\tau,p} \mathbf{x}_{\cdot,j,p} \right] \\ &= \frac{n}{\sigma^2} \mathbb{E} \left[\hat{\beta}_{\tau,p}^2 \right] \\ &\geq \mathbb{E} \left[\arg \max_{k+1 \leq j \leq p} \frac{n}{\sigma^2} \hat{\beta}_{j,p}^2 \mathbb{1}(\mathcal{A}) \right] \\ &= \mathbb{E} \left[\arg \max_{k+1 \leq j \leq p} \frac{n}{\sigma^2} \hat{\beta}_{j,p}^2 \right] - \mathbb{E} \left[\sum_{j=k+1}^p \frac{n}{\sigma^2} \hat{\beta}_{j,p}^2 \mathbb{1}(\mathcal{A}^c) \right]. \end{aligned}$$

Since $n\hat{\beta}_{j,p}^2/\sigma^2 \sim_{\text{IID}} \chi_1^2$ for $k+1 \leq j \leq p$, Lemma A.6 implies that the first term is lower bounded by $\frac{1}{2} \log(p-k)$ for $p-k$ large enough. Applying Cauchy-Schwarz to the second term, we can bound it (in absolute value) from above by

$$(p(p+2))^{1/2} (\pi\sigma^2/n)^{-1/4} \exp(-n/8\sigma^2).$$

Hence,

$$\text{df}(\hat{f}_{k+1,p}) - \text{df}(\hat{f}_{k,p}) \geq \frac{1}{2} \log(p-k) + O(e^{-cn}).$$

Using (51), we get

$$\text{df}(\hat{f}_{k,m,p}) \geq (w_k^{k,m,p} - w_{k+1}^{k,m,p}) \text{df}(\hat{f}_{k+1,p}).$$

Putting everything together, we therefore get

$$\text{df}(\hat{f}_{k,m,p}) - \text{df}(\hat{f}_{k,p}) \geq \frac{1}{2} (w_k^{k,m,p} - w_{k+1}^{k,m,p}) \log(p-k) - k + O(e^{-cn}).$$

Taking a limit as n, m, p go to infinity finishes the proof. \square

Lemma A.6. *Let $Z_1, Z_2, \dots, Z_N \sim_{IID} \chi_1^2$. For N large enough, we have*

$$\mathbb{E} \left[\max_{1 \leq i \leq N} Z_i \right] \geq \frac{1}{2} \log N.$$

Proof.

$$\begin{aligned} \mathbb{E} \left[\max_{1 \leq i \leq N} Z_i \right] &= \int_0^\infty \mathbb{P} \left(\max_{1 \leq i \leq N} Z_i \geq t \right) dt \\ &= \int_0^\infty 1 - \mathbb{P} \left(\max_{1 \leq i \leq N} Z_i < t \right) dt \\ &= \int_0^\infty 1 - \mathbb{P}(Z_1 < t)^N dt \\ &= \int_0^\infty 1 - (2\Phi(\sqrt{t}) - 1)^N dt, \end{aligned} \tag{56}$$

where $\Phi(z)$ is the CDF of a Gaussian distribution. Using the Mills' ratio bound, we have $\Phi(z) \leq 1 - e^{-z^2}$ for z large enough, which would imply that $(2\Phi(z) - 1)^N \leq (1 - 2e^{-z^2})^N$. Since the integrand on the right hand side of (56) is decreasing, we have, for N large enough, that

$$\begin{aligned} \min_{0 \leq t \leq \log N} 1 - (2\Phi(\sqrt{t}) - 1)^N &\geq 1 - (2\Phi(\sqrt{\log N}) - 1)^N \\ &\geq 1 - (1 - 2/N)^N \\ &\geq \frac{1}{2}. \end{aligned}$$

Plugging this lower bound into (56) and integrating from 0 to N completes the proof. \square

Example A.1. We wish to provide an example where RGS reduces training error through the mechanism of avoiding local optima that FS may fall into, as opposed to that of enlarging the hypothesis class. This means that we would like to compare FS to the base estimator of RGS (rather than the ensemble).

In the orthogonal feature setting, for the same value of k , the training loss of the base estimator is worse than FS, since we can do no better than selecting the k features with the

highest correlations with the response. Hence, we make use of a correlated feature setting. The idea, in a nutshell, is to create a regression vector that is strongly correlated with the response, but is not part of the optimal representation. Because of greediness, FS will select this spurious feature, but each base estimator of RGS may have a chance of avoiding its selection if it is omitted from the first candidate set \mathcal{V}_1 .

More rigorously, consider a generative model with features $x_{1,p}, x_{2,p}, \dots, x_{p,p}$. Also assume a feature $x_{0,p}$ which is unavailable for selection, but will be used to define the other features. Suppose that we have $\langle \mathbf{x}_{i,p}, \mathbf{x}_{j,p} \rangle = \delta_{ij}$ for $0 \leq i, j \leq p-1$ and that $x_{p,p} = 3^{-1/2}(x_{1,p} + x_{2,p} + x_{0,p})$, so that $\langle \mathbf{x}_{i,p}, \mathbf{x}_{p,p} \rangle = 3^{-1/2}$ for $i = 1, 2$. Assume $y = \beta(x_{1,p} + x_{2,p}) + \zeta \sum_{i=3}^{p-1} x_{i,p}$. In other words, we have noiseless observations. Assume further that $6^{-1/2}\beta > \zeta > 0$.

Denote the features indices selected by FS (in order) as $\pi(1), \pi(2), \dots, \pi(p)$. Since

$$\langle \mathbf{x}_{i,p}, \mathbf{y} \rangle = \begin{cases} \beta & i = 1, 2 \\ \zeta & 3 \leq i \leq p-1 \\ 2 \cdot 3^{-1/2}\beta & i = p, \end{cases}$$

we have $\pi(1) = p$. Next, the first step residual satisfies

$$\langle \mathbf{x}_{i,p}, \mathbf{r}_1 \rangle = \begin{cases} \beta/3 & i = 1, 2 \\ \zeta & 3 \leq i \leq p-1. \end{cases}$$

Furthermore,

$$\begin{aligned} \|\mathbf{P}_{\mathcal{M}_1}^\perp \mathbf{x}_{i,p}\|^2 &= 1 - \langle \mathbf{x}_{i,p}, \mathbf{x}_{p,p} \rangle^2 \\ &= \begin{cases} 2/3 & i = 1, 2 \\ 1 & 3 \leq i \leq p-1. \end{cases} \end{aligned}$$

Putting these together, the objective for each feature has the value

$$\frac{|\langle \mathbf{x}_{i,p}, \mathbf{r}_1 \rangle|}{\|\mathbf{P}_{\mathcal{M}_1}^\perp \mathbf{x}_{i,p}\|} = \begin{cases} 6^{-1/2}\beta & i = 1, 2 \\ \zeta & 3 \leq i \leq p-1. \end{cases}$$

As such, we have $\pi(k) = k-1$ for $k = 2, 3, \dots, p$. This means that for any $k \geq 3$,

$$\|\mathbf{y} - \hat{\mathbf{f}}_{k,p}\|^2 = (p-k)\zeta^2.$$

We now study the base estimator of RGS, denoted $\check{f}_{k,m,p}$, which depends on a random seed θ . At iteration l , suppose $p \notin \mathcal{M}_l$. Observe that the residual r_l satisfies

$$\frac{|\langle \mathbf{x}_{p,p}, \mathbf{r}_l \rangle|}{\|\mathbf{P}_{\mathcal{M}_l}^\perp \mathbf{x}_{i,p}\|} = \begin{cases} 2 \cdot 3^{-1/2}\beta & \text{if } |\{1, 2\} \cap \mathcal{M}_l| = 0 \\ 2^{-1/2}\beta & \text{if } |\{1, 2\} \cap \mathcal{M}_l| = 1 \\ 0 & \text{if } |\{1, 2\} \cap \mathcal{M}_l| = 2. \end{cases}$$

Hence, if both $x_{1,p}$ and $x_{2,p}$ are selected before $x_{p,p}$, then $x_{p,p}$ is never selected. Denote the feature indices selected by RGS (in order) as $\tau(1), \tau(2), \dots, \tau(p)$. Then $\tau^{-1}(j)$ denotes the step at which feature $x_{j,p}$ was selected. Note that these depend on the random seed θ . We now decompose the probability space into three events. Let

$$\begin{aligned}\mathcal{E}_1 &= \{\tau^{-1}(1), \tau^{-1}(2) \leq \min(\tau^{-1}(p), k)\}, \\ \mathcal{E}_2 &= \{\tau^{-1}(1), \tau^{-1}(2) \leq k\} \setminus \mathcal{E}_1, \\ \mathcal{E}_3 &= (\mathcal{E}_1 \cup \mathcal{E}_2)^c.\end{aligned}$$

We have

$$\|\mathbf{y} - \check{\mathbf{f}}_{k,m,p}\|^2 = \begin{cases} (p-k-1)\zeta^2 & \text{if } \mathcal{E}_1 \text{ holds} \\ (p-k)\zeta^2 & \text{if } \mathcal{E}_2 \text{ holds} \\ (p-k-3)\zeta^2 + C(\theta) & \text{if } \mathcal{E}_3 \text{ holds,} \end{cases}$$

where $|C(\theta)| \leq 2\beta^2$. We next compute bounds for the event probabilities. For $l = 1, \dots, k$, let S_l denote the set of m indices sampled at iteration l . Denote $\gamma = m/p$ as before. By our previous discussion, we have

$$\begin{aligned}\mathbb{P}(\mathcal{E}_1) &\geq \mathbb{P}(1 \in S_1, 0 \notin S_1, 2 \in S_2, 0 \notin S_2) \\ &= \frac{\binom{p-2}{m-1} \binom{p-3}{m-1}}{\binom{p}{m} \binom{p-1}{m}} \\ &= \gamma^2(1 - \gamma^2) + O(1/p).\end{aligned}$$

To compute a bound for $\mathbb{P}(\mathcal{E}_3)$, let us redefine the way S_l is generated as follows: First draw a subset \tilde{S}_l of size m from $[p]$, i.e. including indices that have already been selected. If it contains an index that has already been selected, throw it out and draw it again. Let $W_l^{(j)} = \mathbb{1}(j \in \tilde{S}_l)$ for $j = 1, 2, l = 1, \dots, k$. Then these are Bernoulli random features with probability γ . Note also that if $\sum_{l=1}^k W_l^{(j)} \geq 3$, then $\tau^{-1}(j) \leq k$. We thus have

$$\begin{aligned}\mathbb{P}(\mathcal{E}_3) &= 1 - \mathbb{P}(\tau^{-1}(1), \tau^{-1}(2) \leq k) \\ &= \mathbb{P}(\tau^{-1}(1) > k \text{ or } \tau^{-1}(2) > k) \\ &\leq \mathbb{P}(\tau^{-1}(1) > k) + \mathbb{P}(\tau^{-1}(2) > k) \\ &\leq \mathbb{P}\left(\sum_{l=1}^k W_l^{(1)} < 3\right) + \mathbb{P}\left(\sum_{l=1}^k W_l^{(2)} < 3\right) \\ &\leq 2e^{-k\gamma}(ek\gamma/2)^2,\end{aligned}$$

where the last inequality follows from Chernoff's inequality.

Putting everything together, and using Jensen's inequality, we compute

$$\begin{aligned}\|\mathbf{y} - \hat{\mathbf{f}}_{k,p}\|^2 - \|\mathbf{y} - \hat{\mathbf{f}}_{k,m,p}\|^2 &\geq \zeta^2\mathbb{P}(\mathcal{E}_1) - 2\beta^2\mathbb{P}(\mathcal{E}_3) \\ &\geq \zeta^2(1 - \gamma^2)\gamma^2 - 4\beta^2e^{-k\gamma}(ek\gamma/2)^2 - O(1/p).\end{aligned}$$

For k and p large enough, this last quantity is strictly positive.

B Additional Simulations and Data

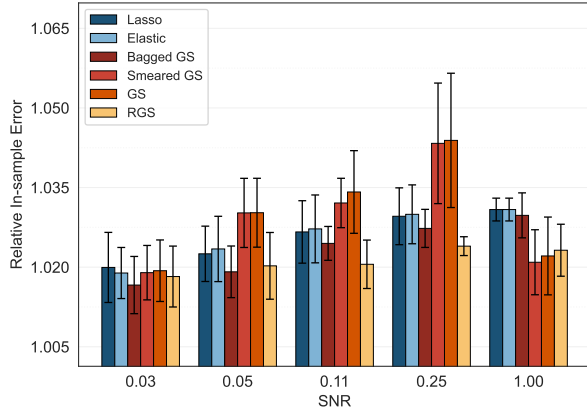
Here, we describe additional simulation results not included in the main paper

B.1 Prediction Performance

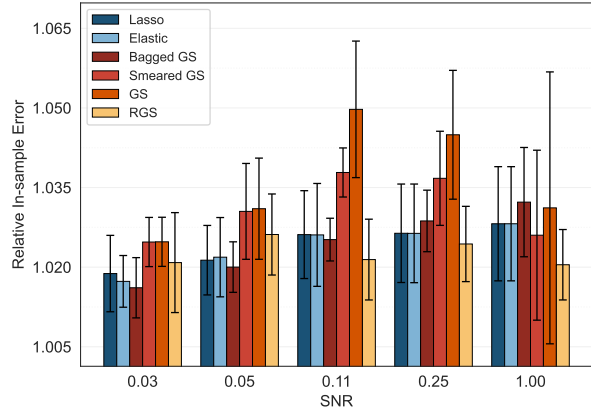
- *Banded correlation.* In Figure 5 and Figure 6 respectively, we present the RISE and RTE results for exact sparsity, banded correlation with $\rho = 0.5$, and aspect ratios $p/n = 0.2, 0.4, 0.5, 0.8$. As observed in the main paper, the increase in aspect ratio seems to slightly magnify the improvement of RGS over other methods.
- *Block correlation.* In Figure 7 and Figure 8 respectively, we present the RISE and RTE results for exact sparsity, block correlation, and aspect ratio $p/n = 0.1$. We set $\Sigma_{ij} = 0.25$ if features $i \neq j$ lie in the same block, and 0 otherwise, with blocks comprising sets of 20 adjacent features. For this setting, RGS does not perform as well as in the banded settings at low SNR. We speculate that this is because the moderately correlated variables that live in the same block are almost indistinguishable when the signal is weak. At low SNR, RGS tends to pick several near-duplicates instead of one strong predictor, which inflates the effective degrees of freedom and mitigates the variance-reduction benefit we observe in the banded experiments.
- *Inexact sparsity.* In Figure 9 and Figure 10 respectively, we present the RISE and RTE results for inexact sparsity, under both banded ($\rho = 0.5$) and block correlation, aspect ratio $p/n = 0.1$. Note that these results mirror the exact sparsity setting quite closely.
- *Varying correlation.* In Figure 11 and Figure 12 respectively, we present the RISE and RTE results for exact sparsity, banded correlation with aspect ratios $p/n = 0.1$, but varying the correlation strength $\rho \in \{0.1, 0.25, 0.5, 0.75\}$. The improvement of RGS over other methods seems to be relatively robust to changes in correlation strength. However, at $\rho = 0.75$ GS and its ensembles no longer vastly outperform lasso and elastic net at high SNR.
- *Heavy-tailed noise.* In Figure 13 and Figure 14 respectively, we present the RISE and RTE results for exact sparsity, banded correlation with $\rho = 0.5$ and block correlation, with aspect ratio $p/n = 0.1$. However, instead of Gaussian noise, we use Laplace noise. The results are similar to the Gaussian noise setting.
- *Model misspecification.* In Figure 15 and Figure 16, we present the results for RISE under a misspecified (nonlinear) model setting. We generate responses via $y_i = \eta g(\mathbf{x}_i) + (1 - \eta)\langle \mathbf{x}_i, \boldsymbol{\beta} \rangle + \varepsilon_i$, where $g(\mathbf{x}_i)$ is a nonlinear function comprising the squared terms and pairwise interactions for the first 5 variables, scaled by $1/\sqrt{p}$. Here, $\eta \in [0, 1]$ is a parameter that controls the degree of nonlinearity and is set at $\eta = 0.5$ in Figure 15 and at $\eta = 0.9$ in Figure 16. $\boldsymbol{\beta}$ follows the exact sparsity design ($\beta_i = 1$ for $1 \leq i \leq 10$ and $\beta_i = 0$ otherwise). SNR is computed via the formula

$$\text{SNR} = \frac{1}{n\sigma^2} \sum_{i=1}^n \left[\eta \left(\sum_{j=1}^5 x_{ij}^2 + \sum_{j=1}^4 \sum_{l=j+1}^5 x_{ij}x_{il} \right) + (1 - \eta) \sum_{j=1}^{10} x_{ij} \right]^2,$$

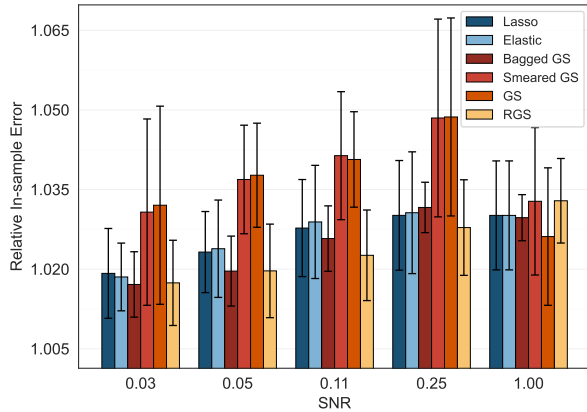
and is varied over the grid $\{0.031, 0.053, 0.11, 0.25, 1.0\}$. We consider both banded correlation with $\rho = 0.5$ and block correlation, with aspect ratio $p/n = 0.1$. We see that RGS performs better than GS and competitively with all other methods across all settings.



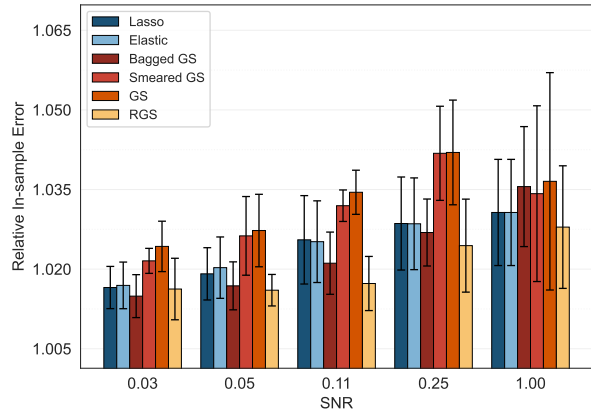
(a) $p/n = 0.2$



(b) $p/n = 0.4$

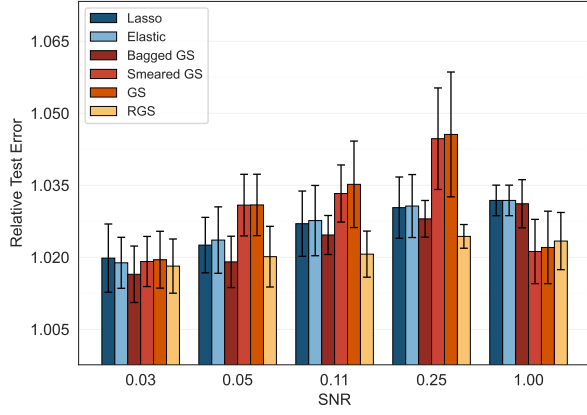


(c) $p/n = 0.5$

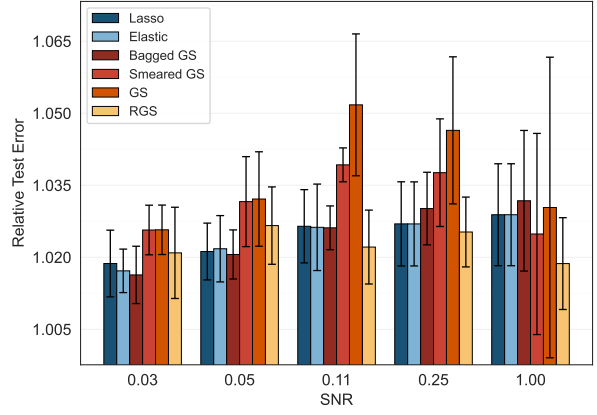


(d) $p/n = 0.8$

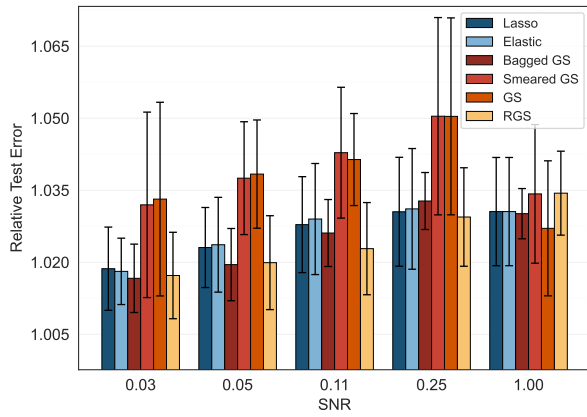
Figure 5: The relative in-sample error across $\text{SNR} \in \{0.031, 0.053, 0.11, 0.25, 1.0\}$ for banded correlated exact sparsity data.



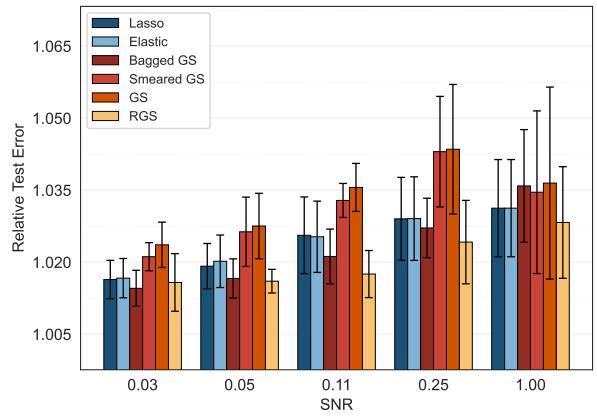
(a) $p/n = 0.2$



(b) $p/n = 0.4$



(c) $p/n = 0.5$



(d) $p/n = 0.8$

Figure 6: The relative test error across $\text{SNR} \in \{0.031, 0.053, 0.11, 0.25, 1.0\}$ for banded correlated exact sparsity data.

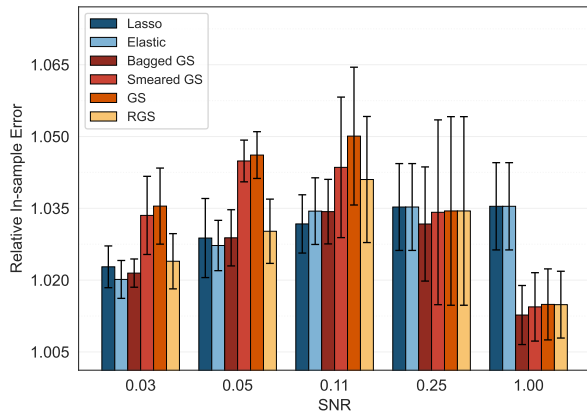


Figure 7: The relative in-sample error across $\text{SNR} \in \{0.031, 0.053, 0.11, 0.25, 1.0\}$ for block correlated exact sparsity data.

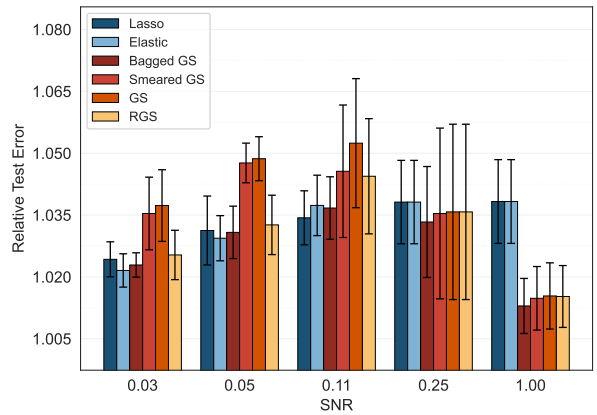
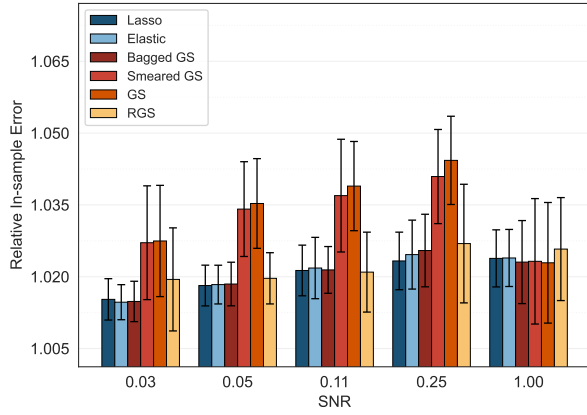
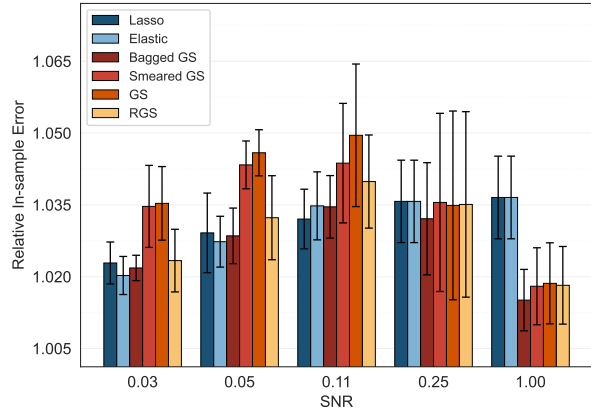


Figure 8: The relative test error across $\text{SNR} \in \{0.031, 0.053, 0.11, 0.25, 1.0\}$ for block correlated exact sparsity data.

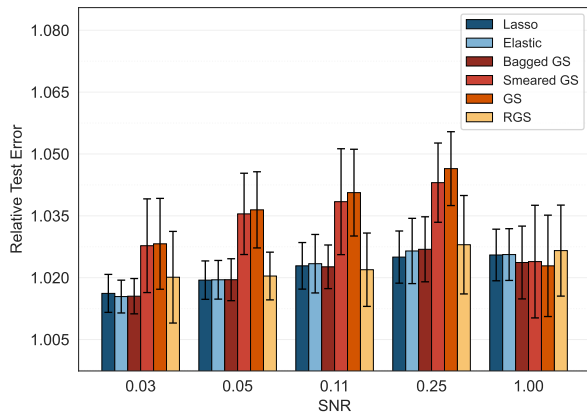


(a) Banded

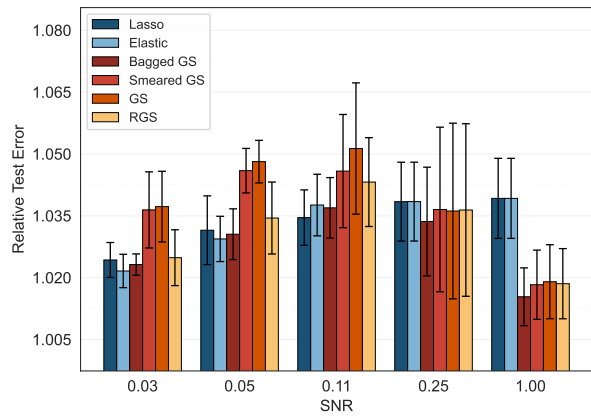


(b) Block

Figure 9: The relative in-sample error across $\text{SNR} \in \{0.031, 0.053, 0.11, 0.25, 1.0\}$ for inexact sparsity data.

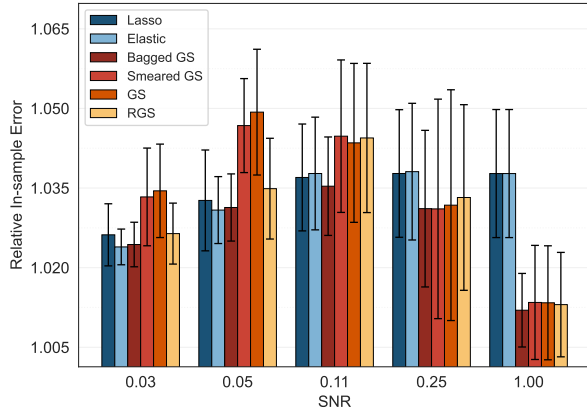


(a) Banded

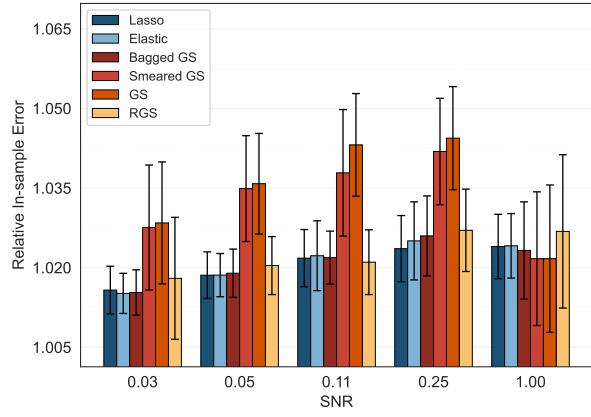


(b) Block

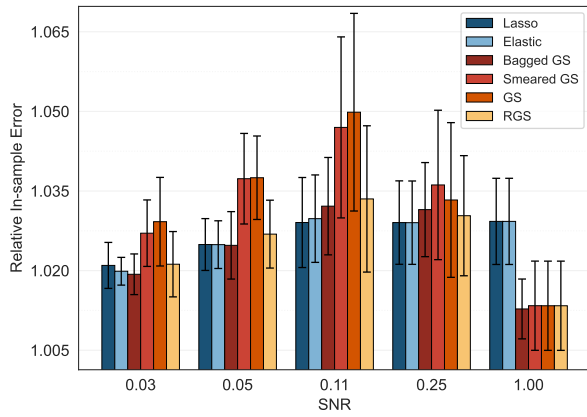
Figure 10: The relative test error across $\text{SNR} \in \{0.031, 0.053, 0.11, 0.25, 1.0\}$ for inexact sparsity data.



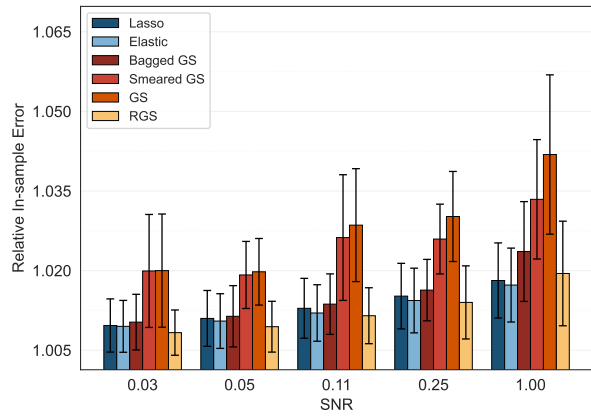
(a) $\rho = 0.1$



(b) $\rho = 0.5$

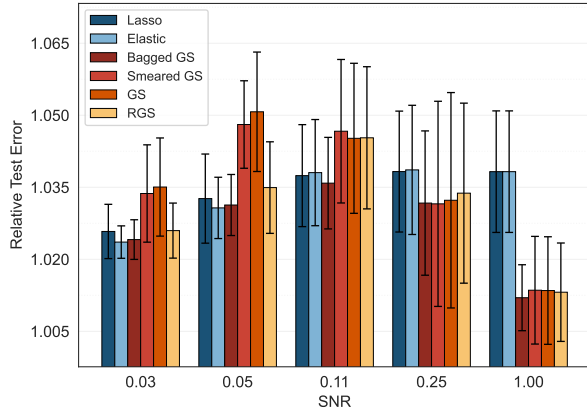


(c) $\rho = 0.25$

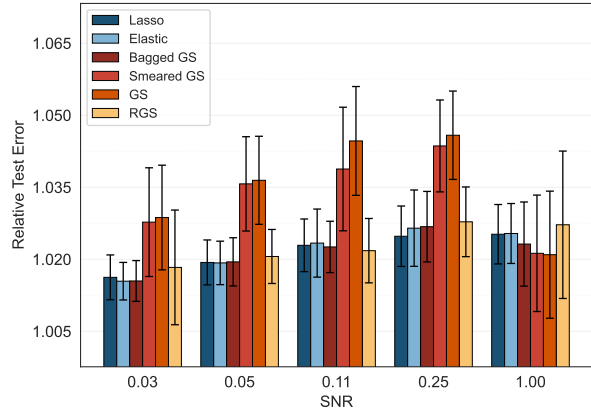


(d) $\rho = 0.75$

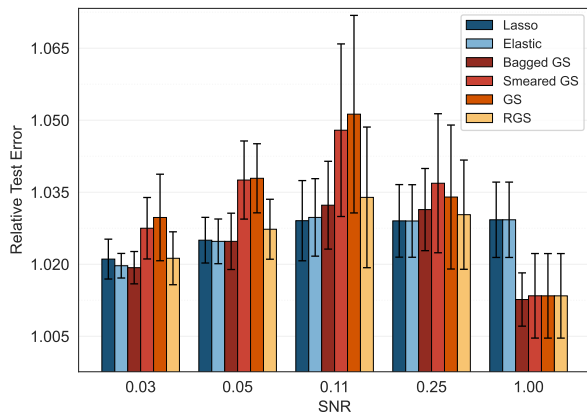
Figure 11: The relative in-sample error across $\text{SNR} \in \{0.031, 0.053, 0.11, 0.25, 1.0\}$ for banded exact sparsity data over various correlation strengths.



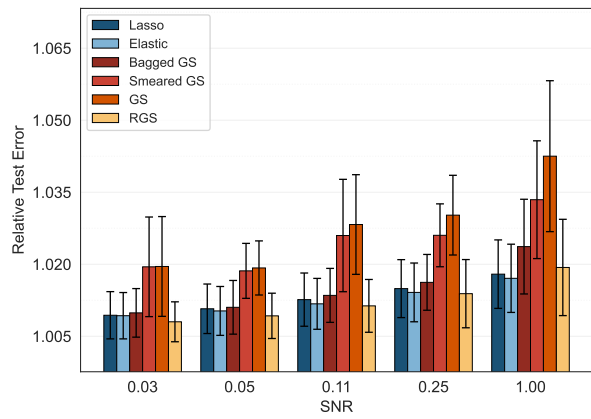
(a) $\rho = 0.1$



(b) $\rho = 0.5$

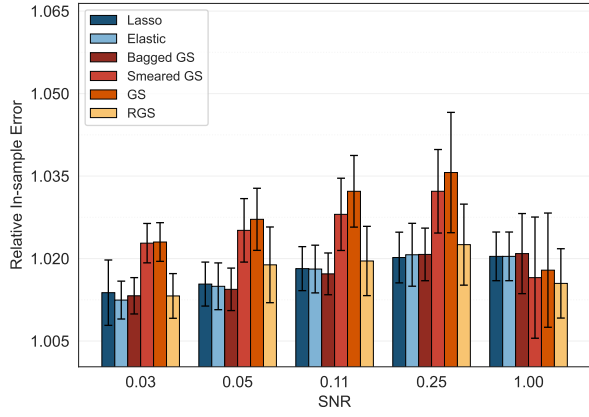


(c) $\rho = 0.25$

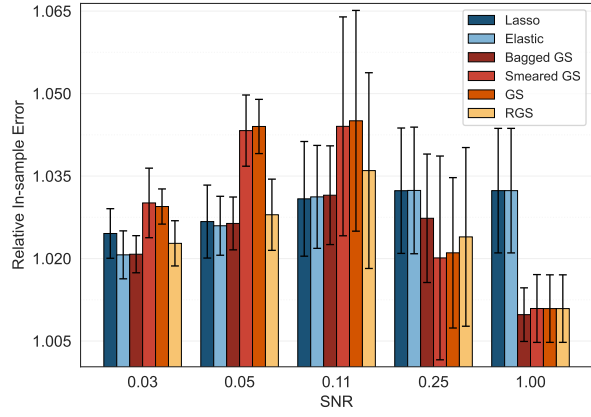


(d) $\rho = 0.75$

Figure 12: The relative test error across $\text{SNR} \in \{0.031, 0.053, 0.11, 0.25, 1.0\}$ for banded exact sparsity data over various correlation strengths.

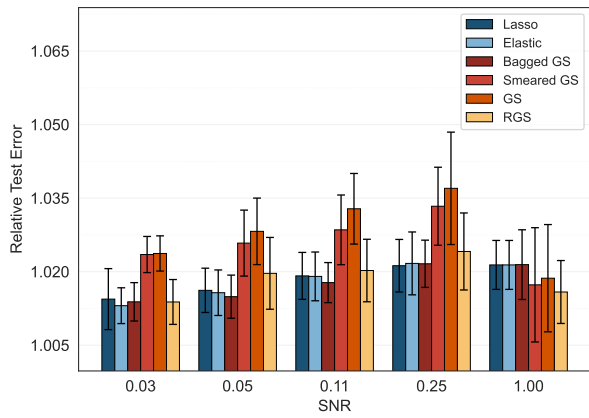


(a) Banded

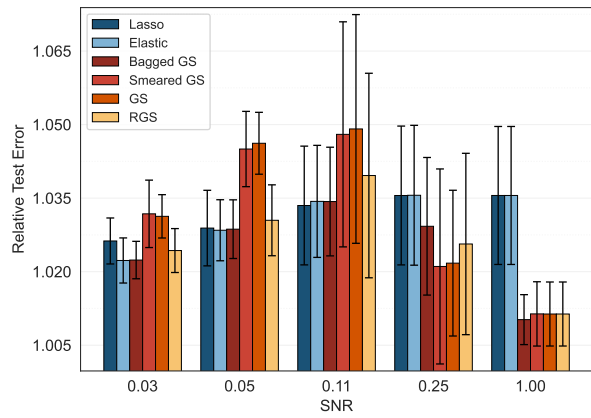


(b) Block

Figure 13: The relative in-sample error across $\text{SNR} \in \{0.031, 0.053, 0.11, 0.25, 1.0\}$ for Laplacian noise.

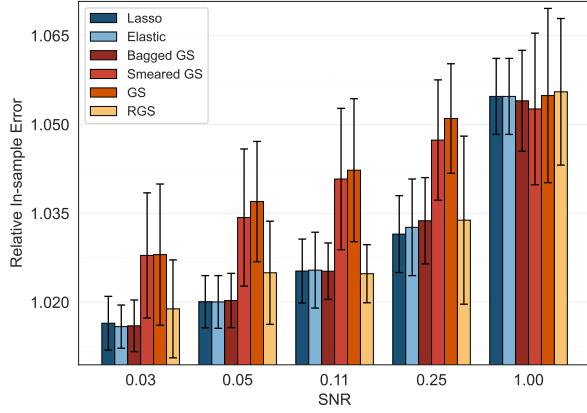


(a) Banded

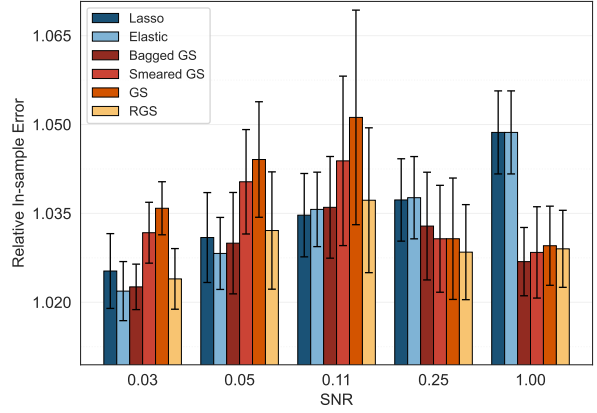


(b) Block

Figure 14: The relative test error across $\text{SNR} \in \{0.031, 0.053, 0.11, 0.25, 1.0\}$ for Laplacian noise.

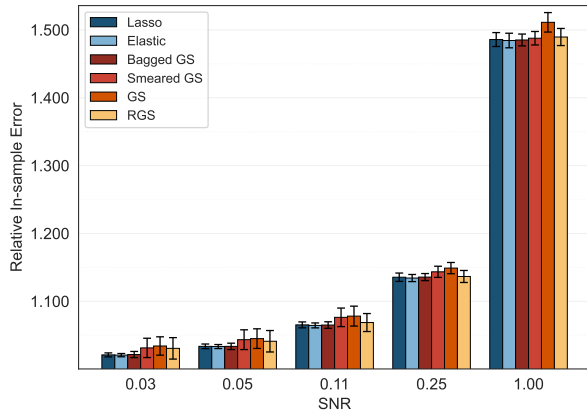


(a) Banded

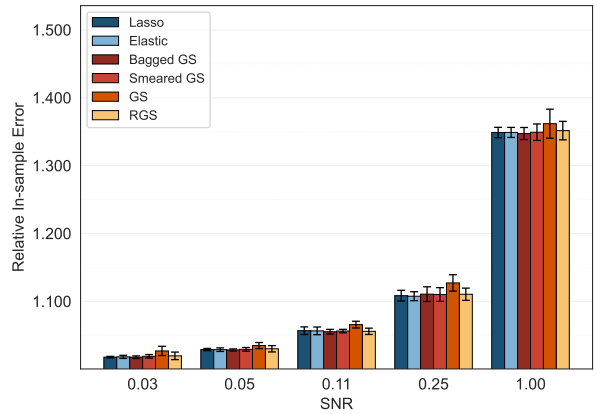


(b) Block

Figure 15: The relative in-sample error across $\text{SNR} \in \{0.031, 0.053, 0.11, 0.25, 1.0\}$ for model misspecification with $\eta = 0.5$.



(a) Banded

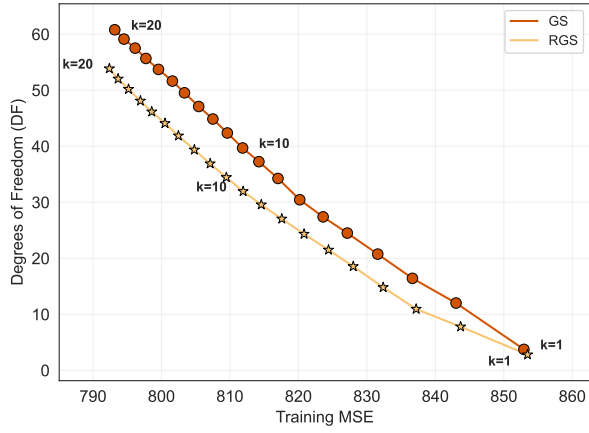


(b) Block

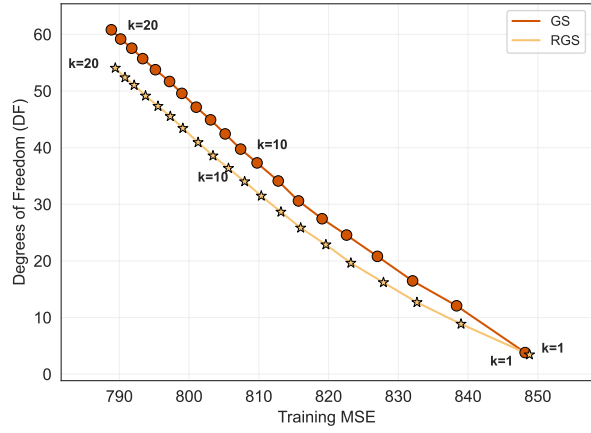
Figure 16: The relative in-sample error across $\text{SNR} \in \{0.031, 0.053, 0.11, 0.25, 1.0\}$ for model misspecification with $\eta = 0.9$.

B.2 Bias-Variance Tradeoff

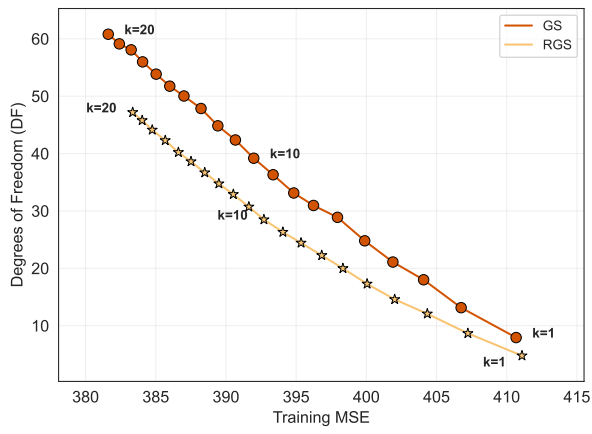
In Figures 17, 18, 19, 20 and 21 respectively, we plot degrees of freedom vs. training MSE for RGS and GS at SNR values 0.031, 0.053, 0.11, 0.5, 1.0. Each figure contains 4 panels, showing the results for (a) banded correlation ($\rho = 0.5$) and exact sparsity, (b) banded correlation and inexact sparsity, (c) block correlation and exact sparsity, (d) block correlation and inexact sparsity. These results suggest that the tradeoff curve for RGS is generally shifted to the bottom left (relative to that of GS), with the shift being more significant at lower SNR settings and for banded correlation. For block correlation, RGS may even have larger degrees of freedom than GS for the same k , which is in accordance with its poor relative performance in Figure 7 and Figure 8.



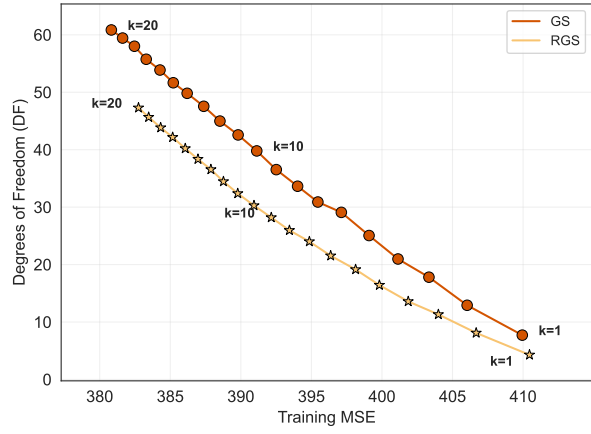
(a) Banded Exact



(b) Banded Inexact

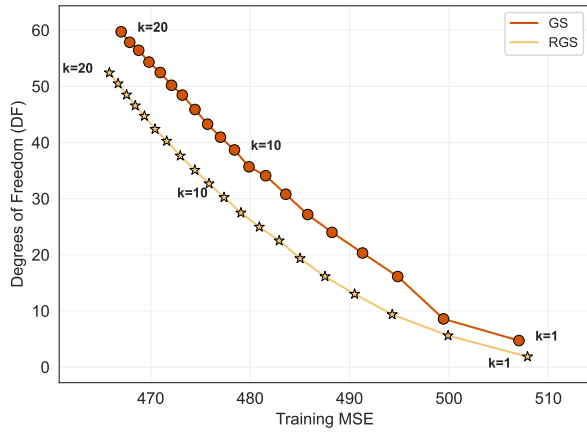


(c) Block Exact

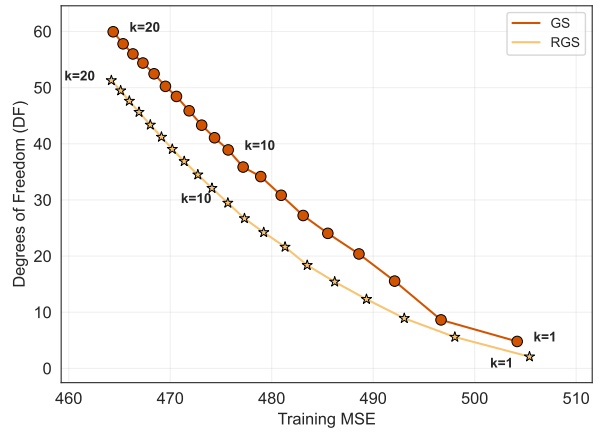


(d) Block Inexact

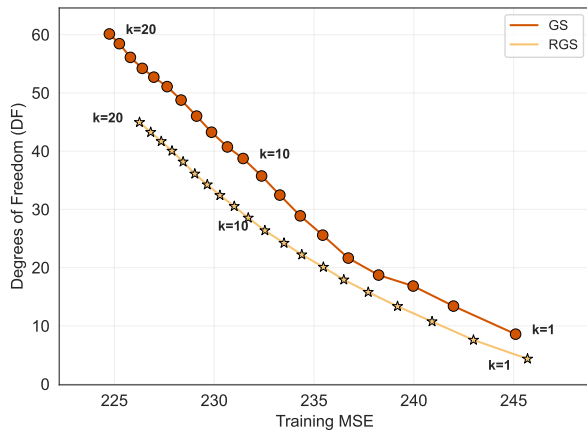
Figure 17: The degrees of freedom for $\text{SNR} = 0.031$ for various correlation and sparsity settings.



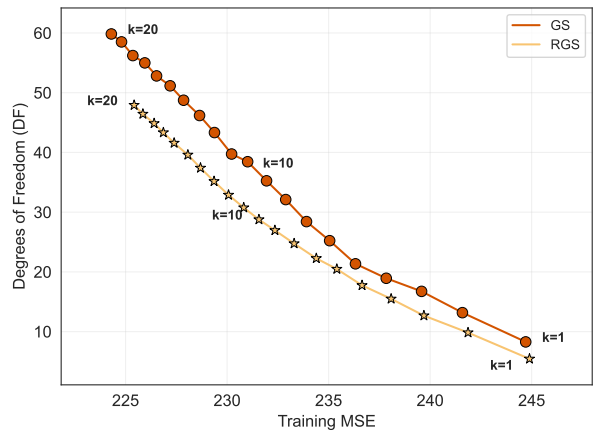
(a) Banded Exact



(b) Banded Inexact

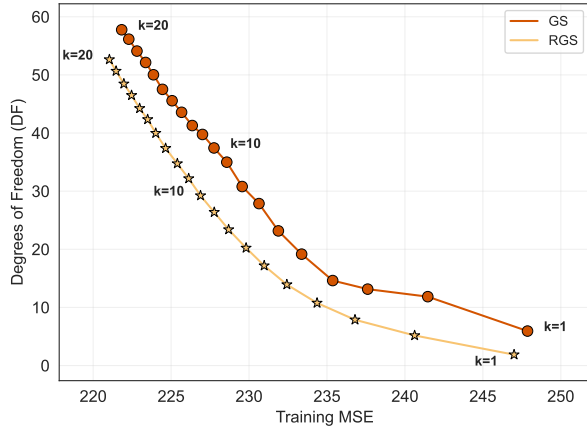


(c) Block Exact

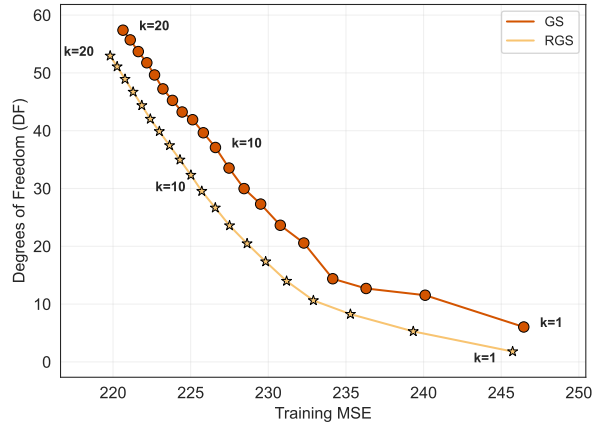


(d) Block Inexact

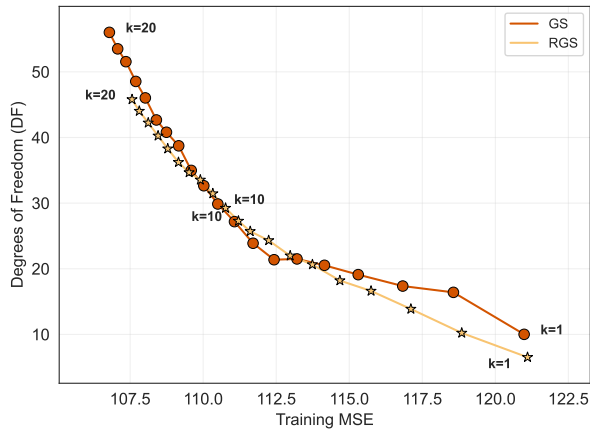
Figure 18: The Degrees of Freedom for $\text{SNR} = 0.053$ for various correlation and sparsity settings.



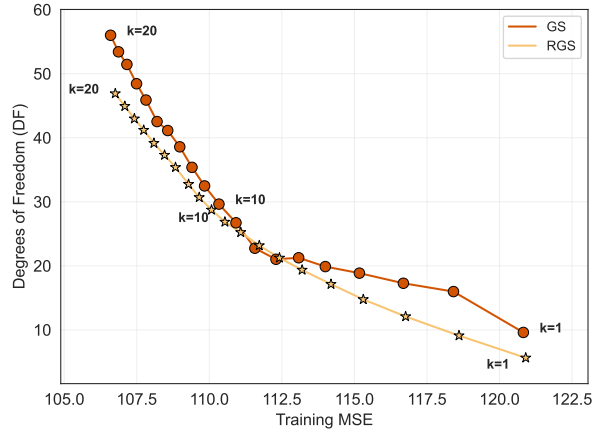
(a) Banded Exact



(b) Banded Inexact

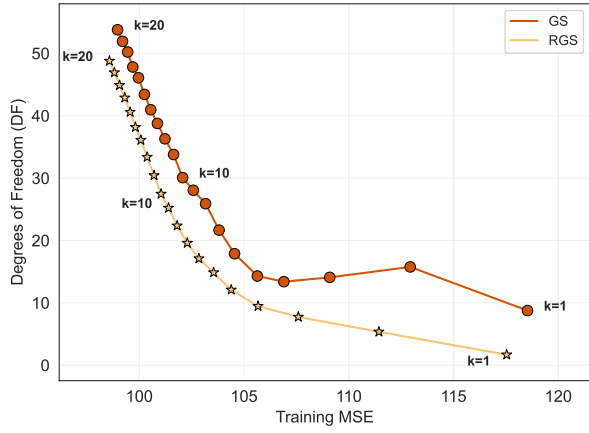


(c) Block Exact

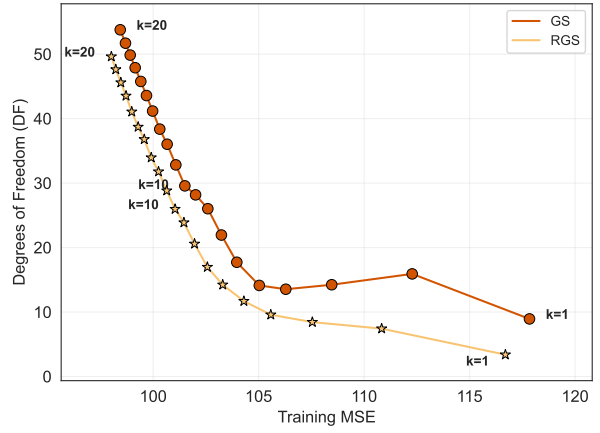


(d) Block Inexact

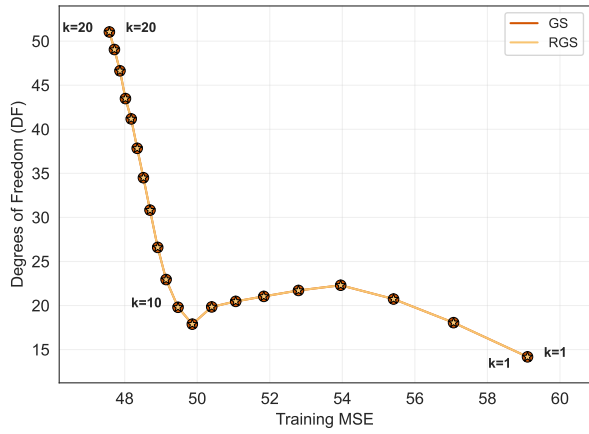
Figure 19: The degrees of freedom for $\text{SNR} = 0.11$ for various correlation and sparsity settings.



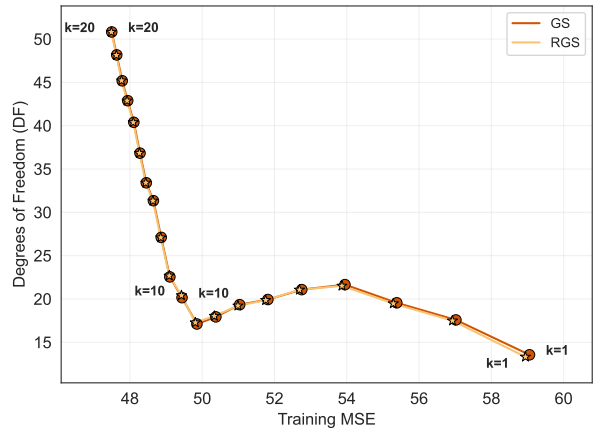
(a) Banded Exact



(b) Banded Inexact

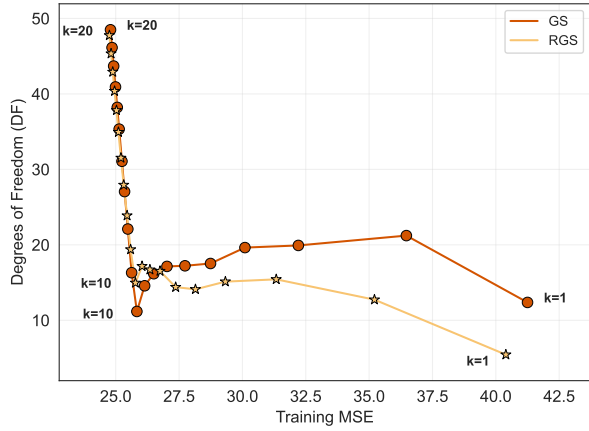


(c) Block Exact

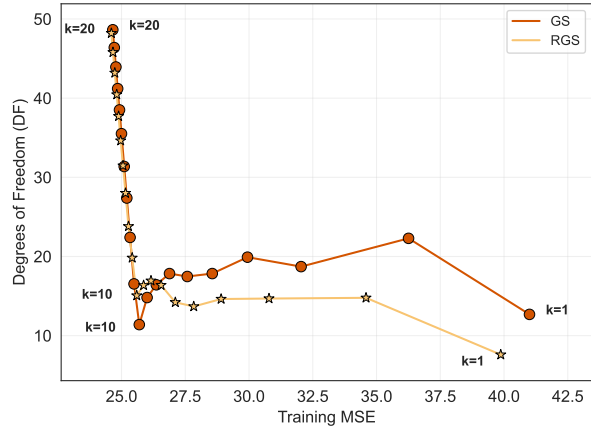


(d) Block Inexact

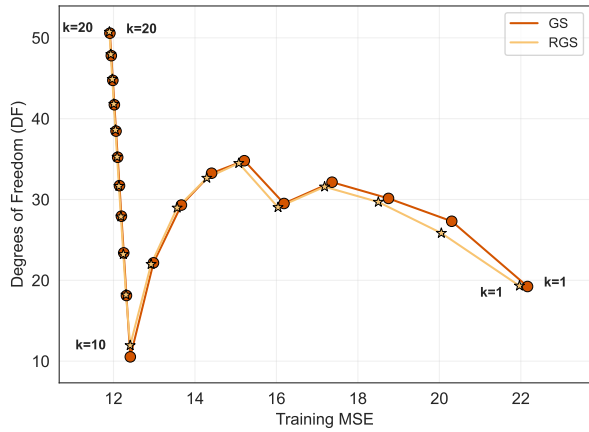
Figure 20: The Degrees of Freedom for $\text{SNR} = 0.25$ for various correlation and sparsity settings.



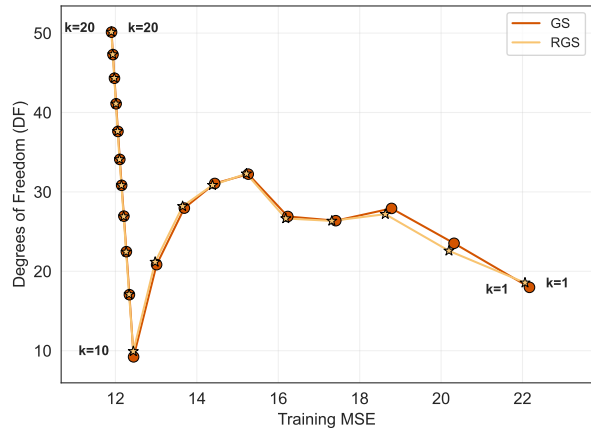
(a) Banded Exact



(b) Banded Inexact



(c) Block Exact



(d) Block Inexact

Figure 21: The degrees of freedom for $\text{SNR} = 1.0$ for various correlation and sparsity settings.